

Here is a sample chapter  
from this book.

This sample chapter is copyrighted and made available for personal use only. No part of this chapter may be reproduced or distributed in any form or by any means without the prior written permission of Medical Physics Publishing.

---

# 12 Patient Immobilization and Image Guidance

---

*“There was a general acknowledgment that anatomic motion was abhorrent, but change is on the way with 4-D and adaptive therapy during imaging, planning and treatment.”*

*(Paul Keall, 2007 private communication)*

## 12.1 Introduction

The ultimate goal of radical radiotherapy is to deliver a high radiation dose to a target while minimizing the dose to surrounding healthy tissues. In order to fulfill this aim, it is essential to consider what constitutes the *target* and how to ensure that the target is in the correct location for treatment. The present chapter (section 12.2) commences with a discussion of target volumes as they are developed in the highly influential reports 50 and 62 of the International Commission on Radiological Units and Measurements (ICRU) (ICRU 1993, 1999). An important aspect of target definition is the concept of margins to ensure that the anatomical volume that must be irradiated is actually receiving the correct dose of radiation on every treatment day (or at least on an acceptable number of treatment days). To optimize radiotherapy delivery, it must be the aim to minimize margins as much as possible. This can be achieved by improving patient setup and immobilization, as will be discussed in section 12.3.

However, knowledge also of the target location on every day of treatment will reduce the uncertainty of dose delivery and therefore the margin required for the delivery. This interfraction motion management can be achieved by using image-guided radiation therapy (IGRT), which is discussed in section 12.4. Another important aspect of uncertainty in delivery is the

possible motion of the target during delivery. Accounting for this intrafraction motion is currently an area of intensive research and some aspects of this will be presented in section 12.5.

## 12.2 The ICRU Target Definitions

The ICRU was founded in 1925 with the brief to develop quantities and units for radiation as well as to establish methods for their measurements and provide the physical data required for this process. The ICRU works now in several technical areas, one of them being radiotherapy. There are important ICRU publications on dosimetry such as the report 64 on radiation beam calibration (ICRU 2001; compare also chapter eight). However, the most influential publications of the ICRU for radiotherapy have been concerned with “Prescribing, Recording and Reporting.” This information was covered briefly in chapter six, section 6.9. We delve into it in more detail in this chapter.

These publications provide a uniform system of volumes and concepts for dose reporting in brachytherapy (ICRU 1985, 1998) and external beam radiotherapy (ICRU 1993, 1999, 2004). These publications are centered on the concept of several target volumes as first introduced by ICRU report 50 and illustrated in figure 12.1, such that:

- i) The *gross tumor volume (GTV)* is the detectable extent of a tumor. Metastases and lymph nodes, which are demonstrably involved, e.g., by PET imaging, are part of the GTV. The GTV is considered the volume of highest density of malignant cells.
- ii) The GTV is surrounded by a *clinical target volume (CTV)* which contains local sub-clinical spread. The density of the tumor cells is typically assumed to reduce with distance from the GTV as demonstrated in the case of breast cancer by Holland et al. (1985). Unlike the GTV, the CTV is determined anatomically not by imaging the tumor itself. If the tumor has been removed by surgery, no GTV exists and the CTV becomes the primary target in adjuvant radiotherapy.
- iii) The *planning target volume (PTV)* is a geometric volume around the CTV. The expansion from CTV to PTV involves a margin that depends on the uncertainty of being able to direct the radiation beam to the target. Uncertainties arise from two distinct sources: motion and deformation of the target and the ability to position the target reproducibly in the radiation beam. The ICRU coins the terms internal margin and set-up margin for the uncertainties attributable to the target and patient setup, respectively (ICRU 1999). This concept is illustrated in figure 12.2. It is important to note that if the magnitude of these margins change randomly, then the two margins should be added in quadrature, hence

$$IMSM_{combined} = \sqrt{IM^2 + SM^2}. \quad (12.1)$$

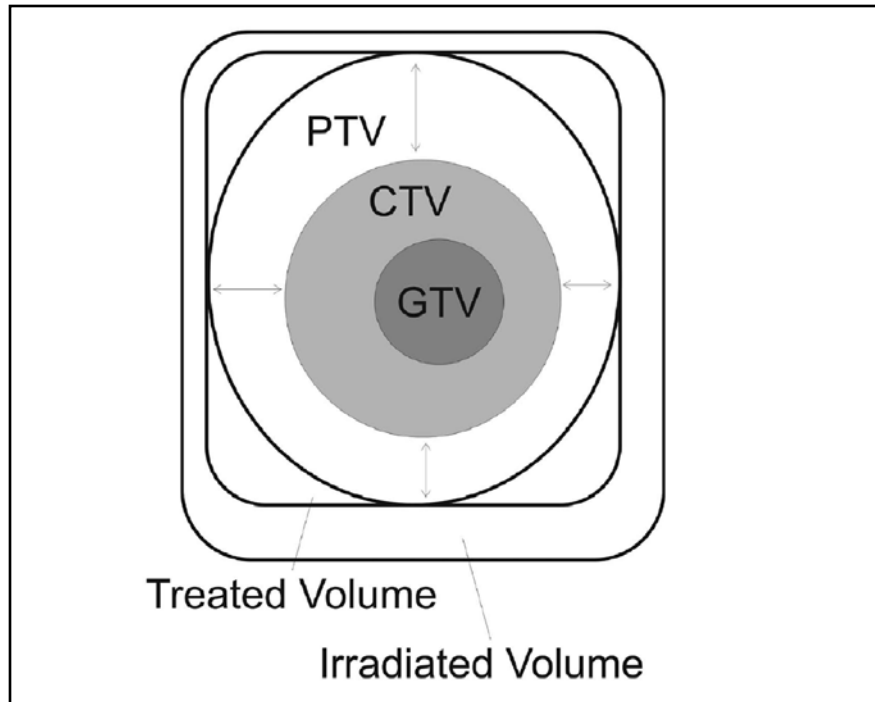


**Figure 12.1:** Schematic illustration of different volumes used for prescribing and reporting dose. PTV = planning target volume; CTV = clinical target volume; GTV = gross tumor volume. (Adapted from ICRU report 50 [1993].)

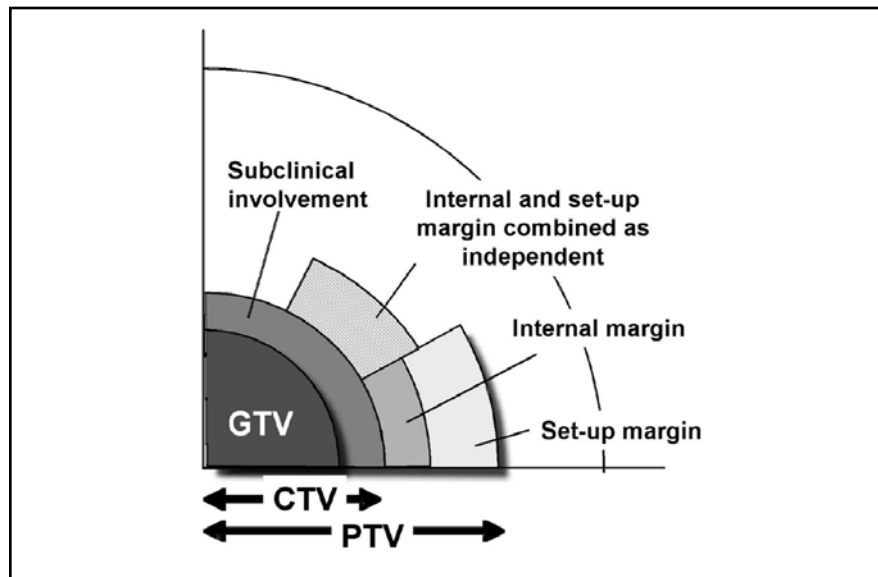


**Figure 12.2:** Schematic illustration of different target volumes and margins. PTV = planning target volume; CTV = clinical target volume; GTV = gross tumor volume. (Modified from ICRU [1999].)

- iv) While PTV margins are typically applied without distinguishing between internal and set-up margin, it is at least in principle possible to determine the internal margin by using time-resolved imaging, such as four-dimensional CT (4DCT) scanning (Rietzel et al. 2005, Hugo et al. 2007). This allows the creation of an *internal target volume (ITV)* (ICRU 1999). The concept has been used successfully for lung (Jin et al. 2006) and esophageal cancer (Lorchel et al. 2006). It is important to note that short time-resolved imaging does not account for changes that occur over longer time intervals, such as organ deformation due to swelling or organ filling (e.g., bladder and rectum in prostate radiotherapy). Serial scans over intervals of hours or days can be used for this purpose—in particular for determining systematic and random error in organ position. It is important to note that the margins around the different target volumes do not need to be symmetric; however, they always have to be considered in 3-D. For example a margin may be created by expanding the CTV using directions normal to its surface, but with an expansion along each direction that depends on the direction.

### 12.2.1 Irradiation Volumes

In addition to these target volumes, the ICRU defines two volumes that indicate which volume in the patient is actually receiving dose. Even with the best IMRT delivery techniques it is not possible to confine the high-dose region entirely to the PTV. As such, the *treated volume (TV)* encompasses the total volume that receives at least a dose required to achieve the treatment aim (best possible tumor control probability while maintaining acceptable complication probability). This dose level could be, for example, the prescription dose or the minimum dose to the target volume. Once a reference dose level is chosen, it is easy to calculate a conformity index such as that described by Knoos et al. (1998):

$$CI = \frac{V_{PTV}}{TV}. \quad (12.2)$$

A conformity index (CI) of 1.0 would indicate that the same total volume is covered by the prescription dose as by the PTV. Note however that the actual region in space corresponding to each volume is, in general, not identical even if  $CI = 1.0$  (the prescription dose volume may be a different shape to, or offset from, the PTV), so the dose distribution must be examined along with taking note of the CI value.

In addition to this, the ICRU defined the *irradiated volume (IV)* as the volume receiving a dose that is considered significant in relation to normal tissue tolerance (ICRU 1999). The dose level used to define the irradiated volume will vary with treatment scenario.

### 12.2.2 Organs at Risk

The more recent ICRU reports on prescribing, recording, and reporting radiotherapy, ICRU report 62 (1999) and ICRU report 71 (2004) extend the

original concept of target volumes explicitly to organs at risk (OAR). The OARs—or critical normal structures as they are often referred to—are “normal tissues...whose radiation sensitivity may significantly influence treatment planning and/or prescription dose” (ICRU 1999). The actual tolerance doses and volume effects concerning these tissues are discussed in more detail in chapter fourteen. The ICRU extends the idea of margins to the OARs. Therefore, a *planning organ at risk volume (PRV)* is derived from the OAR in the same way as the PTV is derived from the CTV.

The concept of PRVs has not yet been generally accepted into radiotherapy treatment planning. While several groups found it useful for spinal cord (Breen et al. 2006) and intestines (Muren et al. 2005, Hysing et al. 2006), there is still some discussion about its usefulness in clinical practice (Stroom and Heijmen 2006). It is also likely that the approach needs to be varied depending on the type of critical structure.

As both PTV and PRV are geometrical volumes they may overlap with each other and other structures.

### 12.2.3 Margins

When considering figures 12.1 and 12.2 it becomes obvious that one of the aims must be to reduce the PTV margin as much as possible. It is therefore useful to consider all aspects that will impact on these margins:

Evidence suggests that a 7% to 10% change in dose to the target volume may result in significant change in the probability of tumor control (ICRU 1976). Other papers indicate that dose variations with accuracy as low as 5% and as high as 15% may be critical (Brahme 1984, Chappell and Fowler 1994). Mijneer et al. (1987) using normal tissue control probabilities (NTCPs) and Brahme et al. (1988) using TCPs quote required uncertainties of about 7% ( $2\sigma$ ). Considering errors are combined in quadrature, this may be a practical aim within the entire radiotherapy treatment process.

*Internal margins* account for:

- i) Intrafraction organ motion.
- ii) Variations in site, size, and shape of the organs and tissues contained in or adjacent to the CTV (ICRU 1999). A very important element of the internal margin to account for is systematic error in target position. This is the difference between the mean position over the course of treatment and the position determined during planning scans. An inadequate margin for systematic error will mean that part of the CTV will be systematically underdosed.

*Set-up margins* account for:

- i) Patient positioning.
- ii) Dosimetric uncertainties (e.g., positioning of shielding).
- iii) Mechanical uncertainties (e.g., gantry sag, couch sag).
- iv) Differences between planning equipment (CT, simulator) and treatment units.
- v) Human factors (ICRU 1999).

Unfortunately, the distinction between the two margins is not perfect. Set-up variations may lead to variations in organ site and shape. However, set-up margins are mostly a result of interfraction variations, while internal margins include also a large component of intrafraction variation. Modern image guidance also has the capability to reduce some uncertainties affecting both, internal and set-up margin (but not all!). For example, daily CT acquisition of the patient in treatment position allows reduction of internal margin due to determination of organ shape and location while at the same time reducing the uncertainty of setup and patient positioning. As such, it may be increasingly difficult to apply the two margins independently of each other.

### 12.2.4 A Margin Recipe

A so-called *margin recipe* was derived by van Herk et al. (2000). This is used to derive the magnitude of margin to be placed beyond a CTV to obtain a PTV. Derivation of this was based on the random and systematic geometric target position variations and the effects they have on dose coverage of the CTV. It also takes into account the penumbral width of the beam. For a penumbral width of 3.2 mm the margin recipe was expressed as:

$$IMSM_{combined} \approx 1.5\Sigma + 0.7\sigma, \quad (12.3)$$

where  $\Sigma$  is the systematic error and  $\sigma$  is the random error. This margin should only be considered as a *lower limit* for safe radiotherapy as it does not take into account rotational positional variations or shape distortion.

## 12.3 Patient Setup and Immobilization

### 12.3.1 Patient Support Assembly: Couch

Modern linacs such as the one shown in figure 12.3a have a couch top that includes indexing (see figure 12.3b). This consists of simple recesses on the edge of the couch that immobilization devices clip into. This ensures they can be fixed in the same superior, inferior, and lateral locations on the patient couch for each treatment fraction.

#### **Immobilization Devices**

While immobilization aims to provide reproducible patient positioning with minimal patient movement, patient comfort should also be considered; there needs to be a balance between the two aims. Various immobilization devices for use on the linac couch are available; these include:

- i) Head cast and support systems provide fixation predominantly for patients undergoing brain and head and neck radiotherapy treatments. The casts may also be used for upper mantle treatments. The

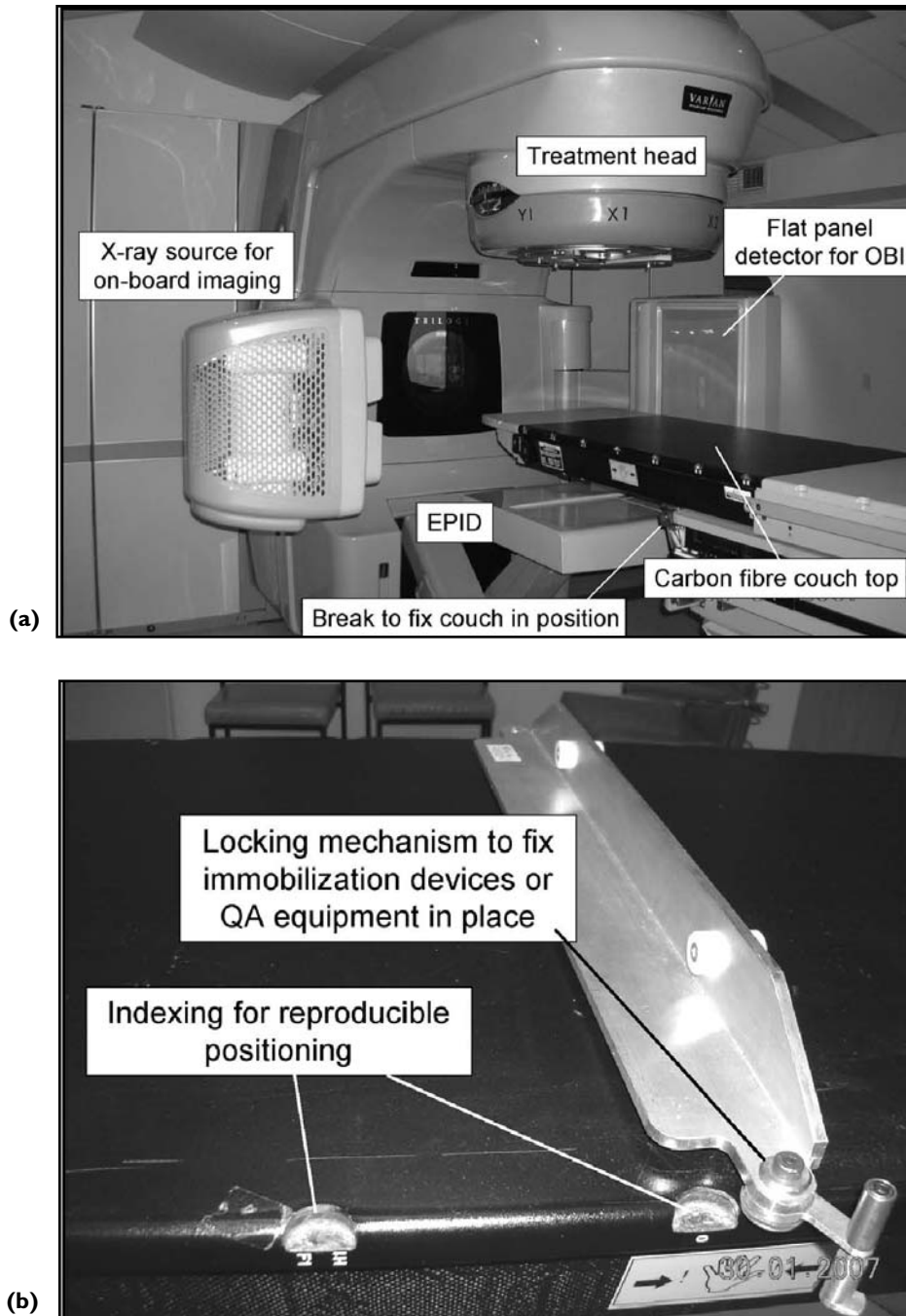
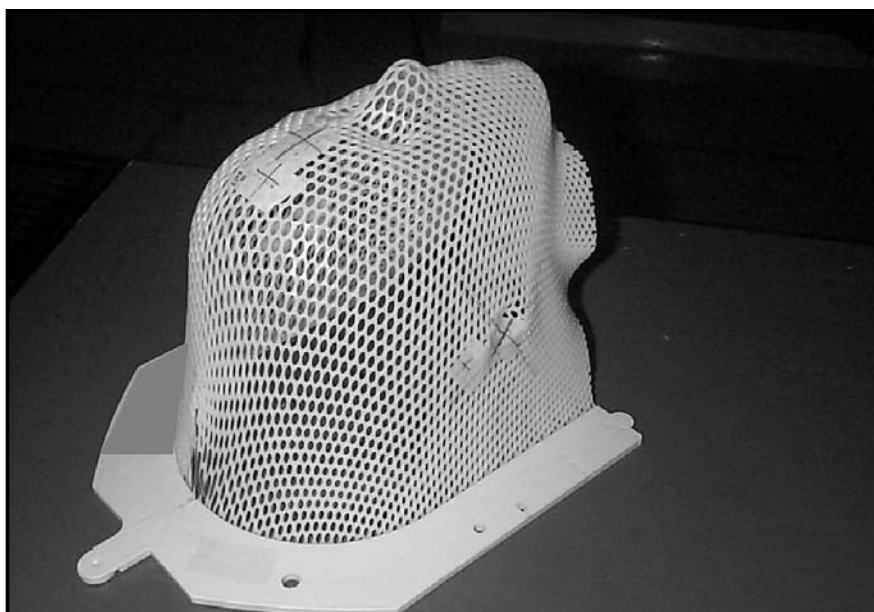


**Figure 12.3:** Linac and couch top indexing. (a) Photograph of a linac with carbon fibre couch top shown in relation to linac treatment head, EPID, On-Board Imager (OBI)™ tube, and flat-panel detector (FPD). (b) Close-up view of couch top and indexing device.

head and chin position may be critical for field matching. The head mask can have various points of attachment to the head mask fixation device and sometimes the mask extends to the shoulder region. Molds are commonly made from thermoplastic Orfit™ material, which molds when heated (see figures 12.4a ,12.4b). Figure 12.4c shows a head and shoulder mask mounted to a head board that extends beyond the end of the linac couch, ideal for multi-field IMRT.

- ii) Vacuum bags and body casts are filled with small polystyrene beads that mold to the patient's shape when evacuated. These reduce pelvic tilt, which can otherwise occur after the first few fractions when the patients tend to be more relaxed during treatment (see figure 12.5a). Body casts are sometimes used for further immobilization (see figure 12.5b).
- iii) Bellyboards for prone positioning (see figure 12.5c) are often used for patients having rectum or other pelvic treatments. The advantage is that the small bowel falls into the gap in the board, away from the treatment volume.
- iv) Breast jigs similar to that shown in figure 12.5d are used to help immobilize the patient and to create a sternum that aligns with the field edge without collimator rotation, thus minimizing the lung irradiated. It is important that patients are CT simulated then treated in the identical jig arrangement (e.g., jig wedge angle needs to be identical).



(a)

**Figure 12.4:** Patient head and neck immobilization devices. (a) Patient head cast. (b) Different head supports. (c) Head and shoulder mask mounted to a head board that extends beyond the end of the linac couch, ideal for multi-field IMRT.

- v) Knee and ankle supports, often used in combination with other fixation devices, ensure reproducible leg position, which seems to help with reproducible setup (see figure 12.5e).

This is a snapshot of the many devices available. The implementation of immobilization strategies into each clinic usually follows a detailed examination of portal (or other) images collected in the linac bunker on the patient just prior to or just after treatment. If the immobilization method is shown to improve setup reproducibility, then it is implemented for routine use on the cohort group of patients for whom it has been shown to be useful.

A higher level of precision of immobilization can be obtained by using stereotactic frames (these are outlined in chapter seven); however they are not always practical for all patients having day-to-day fractionated treatment.

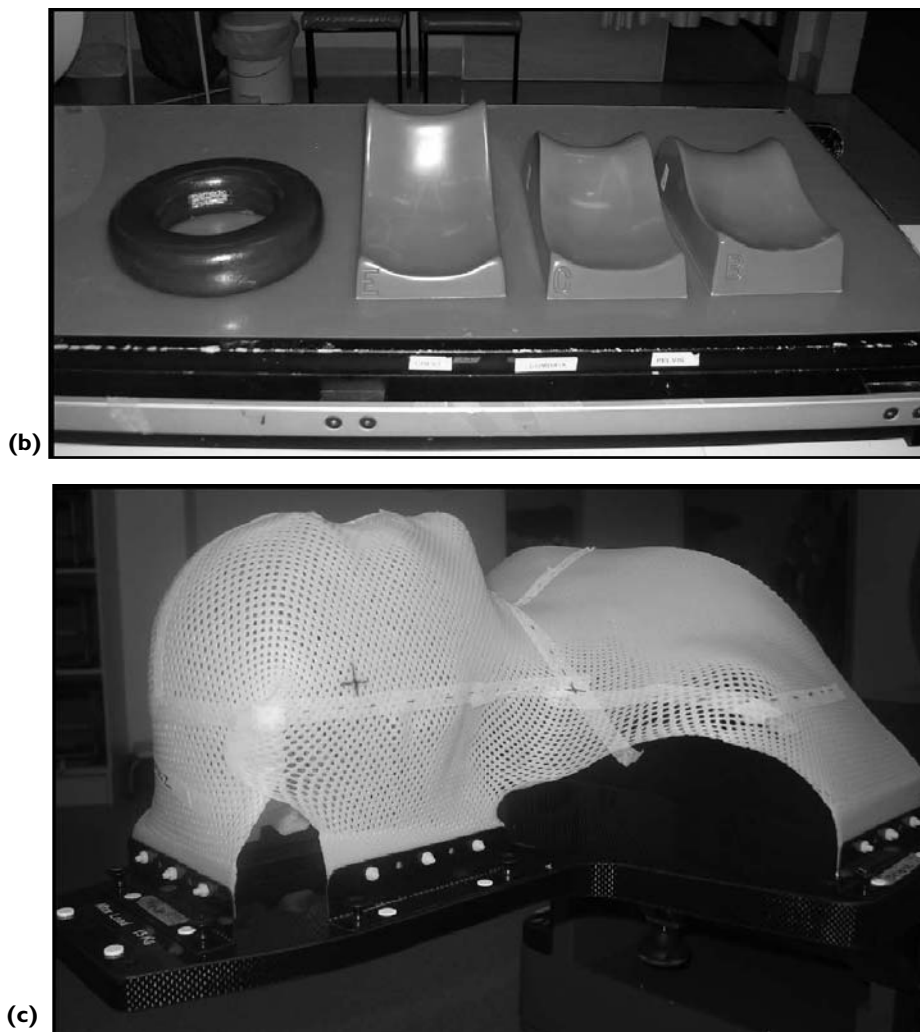
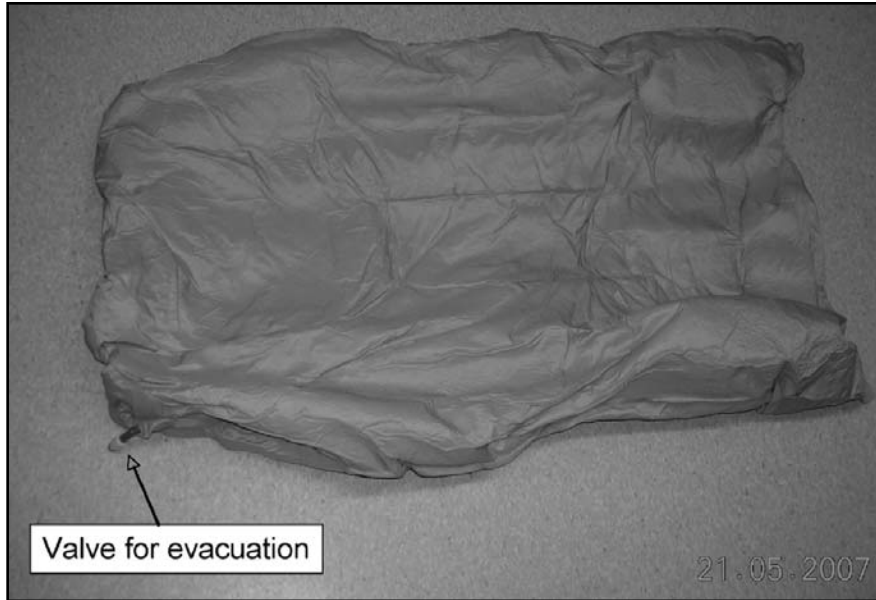


**Figure 12.4:** (Continued.)



(a)



(b)

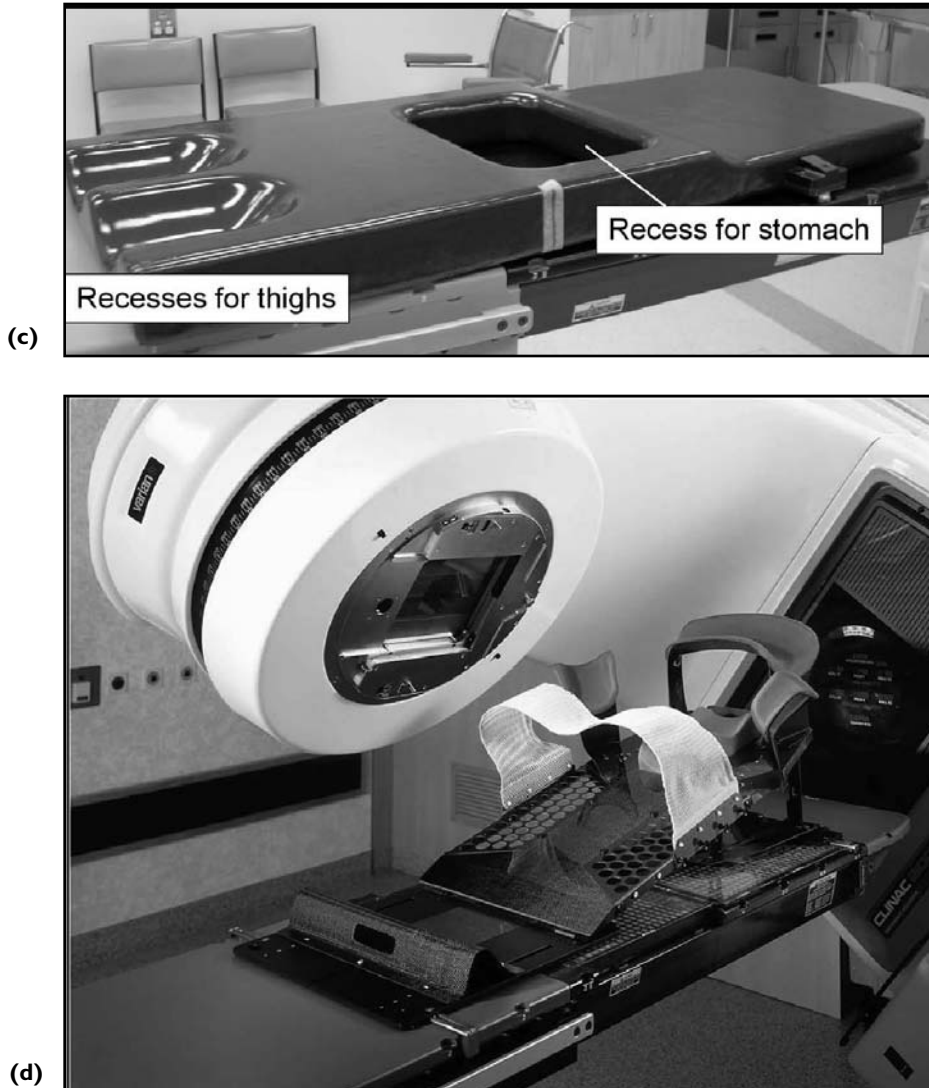


**Figure 12.5:** Patient body immobilization devices: (a) Vac fix bags: These are filled with small polystyrene balls. When the air is removed from the bag while placed under the patient trunk, a solid impression is made of the patient's shape, then the same device with the fixed impression is used as a custom fit for immobilization of patient during each treatment fraction. (b) Body casts, for abdominal immobilization, are not used at all centers but may aid in further immobilization. (c) Bellyboards for prone positioning are often used for patients having rectum or other pelvic treatments. The advantage is that the small bowel falls into the gap in the board, away from the treatment volume. (d) A typical breast jig. This is used to help immobilize the patient and to create a sternum that aligns with the field edge without collimator rotation.

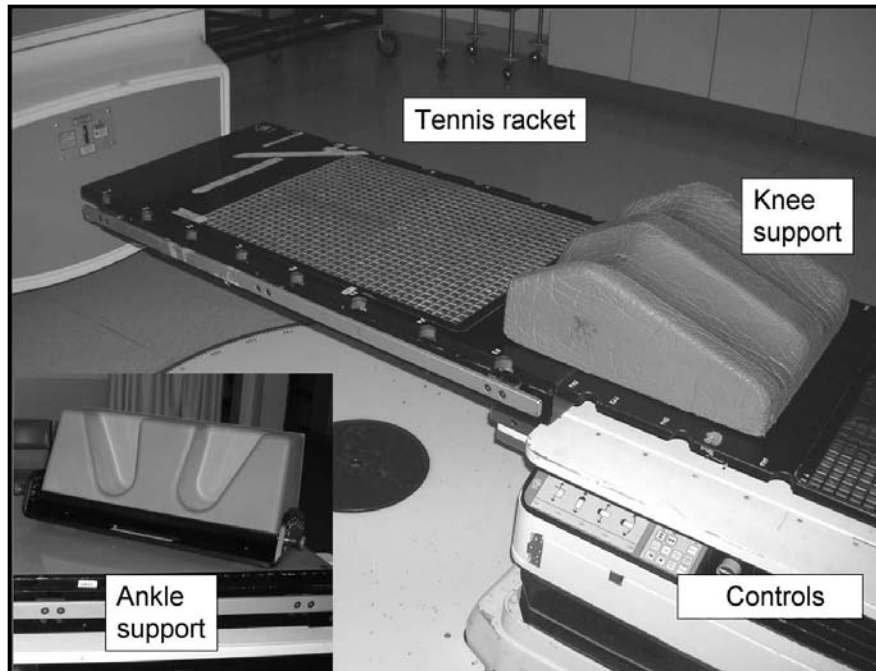


**Figure 12.5:** (Continued.) (e) Patient body immobilization devices: (e) Knee and ankle supports used to ensure reproducible leg and foot position, which, in turn, stabilizes setup in the trunk region.

### 12.3.2 External and Internal Markers

Patients are often aligned to external markers either placed on the head cast or positioned at patient tattoo position. External marker positions are usually defined at CT simulation time, whereby external fiducial markers are placed with reference to isocenter. Unfortunately, there is internal organ mobility so external markers can at best only guide the initial treatment setup. While some structures such as the pelvic lymph nodes may follow the bony anatomy quite nicely, other organs such as the prostate undergo significant motion with respect to the bony anatomy. The extent of this motion is summarized in table 12.1.

It is the verification views using electronic portal imaging devices (EPIDs) or linac-mounted imaging devices (LMIDs) that more and more frequently guides *on-line* correction of position. This can be achieved by small repositioning moves of the linac couch in the  $(x, y, z)$  axis, essentially guiding the center of each treatment beam to isocenter.

Because the images from EPIDs are not ideal for showing soft tissue anatomy, it is possible to place internal fiducial markers in some organs to guide the treatment, as shown in figure 12.6a and 12.6b (e.g., for prostate typically three gold markers are inserted). In this case, isocenter positioning is being based on soft tissue anatomy surrogates. This is a major mind shift

**Table 12.1:** Mean and standard deviation (SD) of prostate movements from various reports in the literature. Movements are in centimeters (cm) and axis moves are classified as anterior-posterior, superior-inferior, and left-right

Patients	Method	Ant-Post (cm)		Sup-Inf. (cm)		Left-right (cm)		Reference	Comments
		Mean	SD	Mean	SD	Mean	SD		
55	Fiducial markers	0.56 (post)	0.41	0.59 (inf.)	0.5	0.05	0.15	Crook et al. (1995)	Treated supine
50	CT	0.2 (post)	0.29	0.05 (inf.)	0.33	0.06 (left)	0.08	Zelevsky et al. (1999)	Large deviations linked to large bladder and rectal volumes.
6	Ultrasound	0.5	0.4	0.3	0.4	0.3	0.3	Chinnaiyan et al. (2003)	Post prostatectomy
10	Ultrasound	0.4	0.3	0.4	0.4	0.4	0.3	Chinnaiyan et al. (2003)	No prostatectomy
23	Fiducial markers		0.44		0.37		0.24	Nederveen et al. (2003)	Off-line target position verification allowed reduced margins.
13	Fiducial markers		Base 0.29 (ant.) Apex 0.21 (sup.)		Base 0.21 (sup.) Apex 0.21 (sup.)			Wu et al. (2001)	
35	BAT and Portal images	0.13	0.57	0.16	0.64	0.09	0.33	Little et al. (2003)	Comparison between BAT + Portal imaging.



**Figure 12.6:** Internal fiducial markers. (a) Rando phantom with fiducials showing MV compared with kV beam's-eye view image. (Courtesy of R. Amner.) (b) Rando phantom kV CT image showing three internal gold fiducials. (Courtesy of R. Amner.) (c) Breast phantom showing visibility of surgical clips. (Courtesy of D. Willis.)

away from alignment to bony landmarks, which many centers have traditionally used.

Surgical clips in breast cancer patients can also act as good potential fiducial markers (see figure 12.6c). In other organs it is more difficult to place internal markers without risk of other complications (e.g., lung).

## 12.4 Interfraction Motion Management: Image Guidance

Several new developments have helped us monitor movement of bony anatomy and soft tissue surrogates within the patient in the linac room. With the exception of EPIDs or port films, which can gather images during treatment, all the other more recent linac add-on devices can monitor patient position just prior to treatment. Image guidance tools that are available include:

- i) *EPIDs*. Because they collect image data using the linac's megavoltage beam, with a detector that is relatively insensitive to these energies, they generally give the lowest quality images of this group. They do however work reasonably well with fiducial marker surrogates (see figure 12.6a). While they are able to acquire images through the course of treatment, they are more routinely used to take a snapshot beam's-eye view (BEV) requiring about 2 monitor units just prior to treatment.



**Figure 12.7:** Two orthogonal kV images (i.e., two images taken 90° gantry rotation separating the image) acquired using a Varian OBI™ to be used for 3-D patient positioning. SEE COLOR PLATE 53.

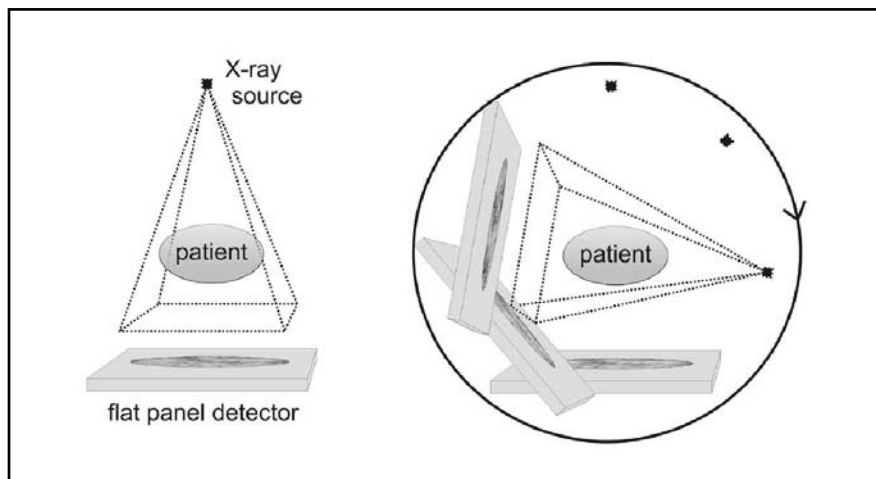


**Figure 12.8:** Schematic illustration of cone beam CT acquisition principle. The x-ray source and FPD rotate  $360^\circ$  and a pyramidal cone beam is used to acquire the information, whereas in conventional fan beam CT a narrow slit (in the superior-inferior direction) is used. This reduces scatter effects.

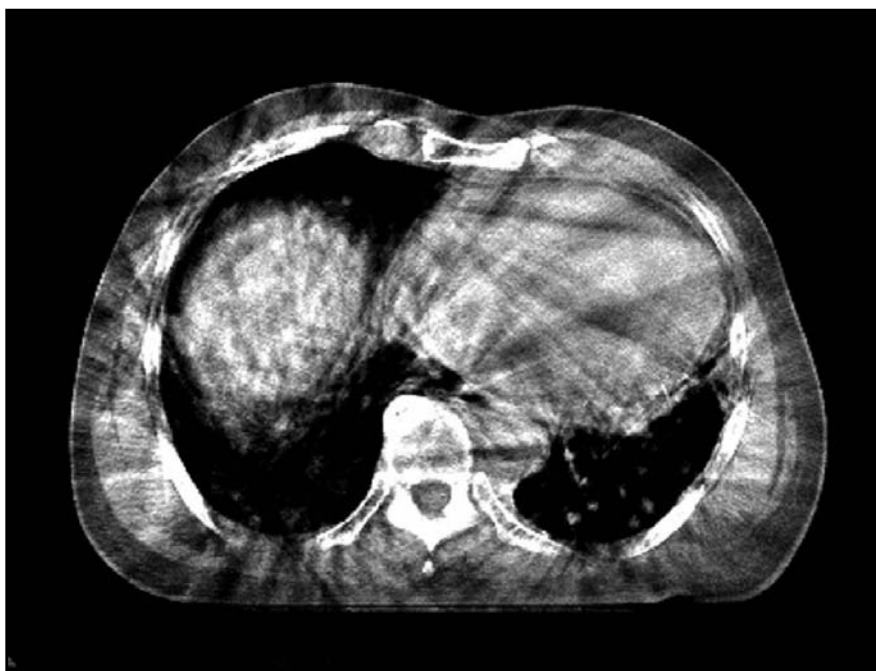


**Figure 12.9:** Cone beam CT image affected by motion artifacts; lung acquisitions show movement artifacts due to the slow rotation required for the open gantry to acquire the data during several breathing cycles.

- ii) *LMIDs*. kV x-ray BEV images taken orthogonal to each other (90-degree gantry rotation between images) are shown in figure 12.7. With these images 3-D patient repositioning using couch moves can be undertaken using *on-line* fraction-by-fraction correction just prior to treatment. The other option is *off-line* correction after analyzing the data for several fractions (See et al. 2000). The bony landmarks show up well, but soft-tissue surrogates such as gold seeds are still probably required for prostate positioning.
- iii) *kV cone-beam CT imaging*. This is achieved by rotation of the LMID around the patient using up to a 360-degree gantry rotation. The principle is explained in figure 12.8. Reasonable images are achievable in prostate (see figure 1.23) and head and neck sites. Because of the open gantry design rotation is legally restricted to between 45 and 60 seconds, so there are motion artifacts in some sites, especially in lung as shown in figure 12.9. Vendors that supply options ii and iii are Varian Medical Systems and Elekta.
- iv) *CT-on-Rails*. As shown in figure 12.10, a CT scanner is mounted at the end of the linac couch and a 180-degree couch rotation, with the patient on couch, is then required before treatment. The device offers fan beam kilovoltage (diagnostic) quality CT scans. The vendor that offers this option is Siemens Medical Solutions.

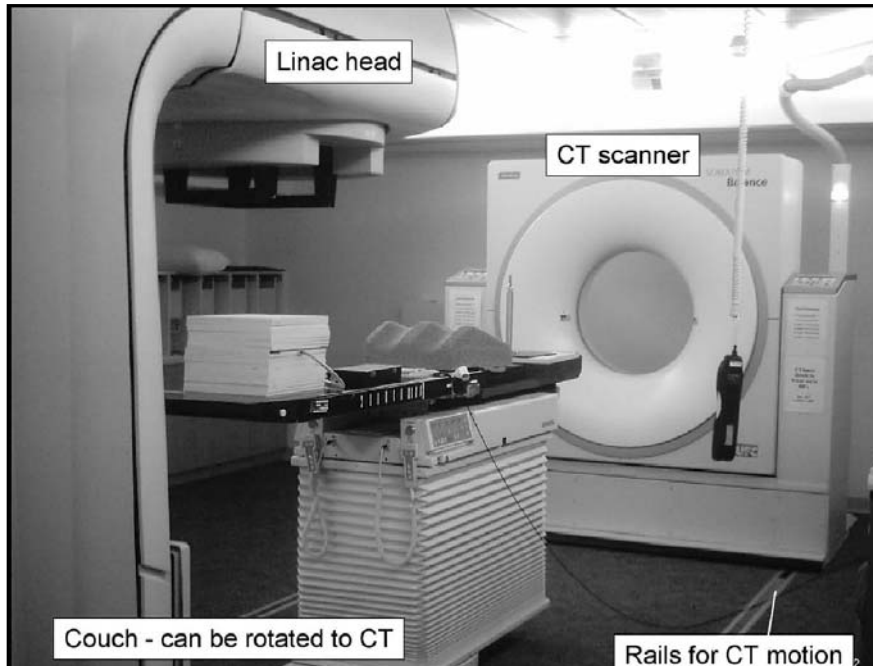


**Figure 12.10:** CT-on-Rails in linac room, mounted at end of linac couch. Patient has CT just before treatment, then a 180° rotation of couch enables patient treatment by linac.

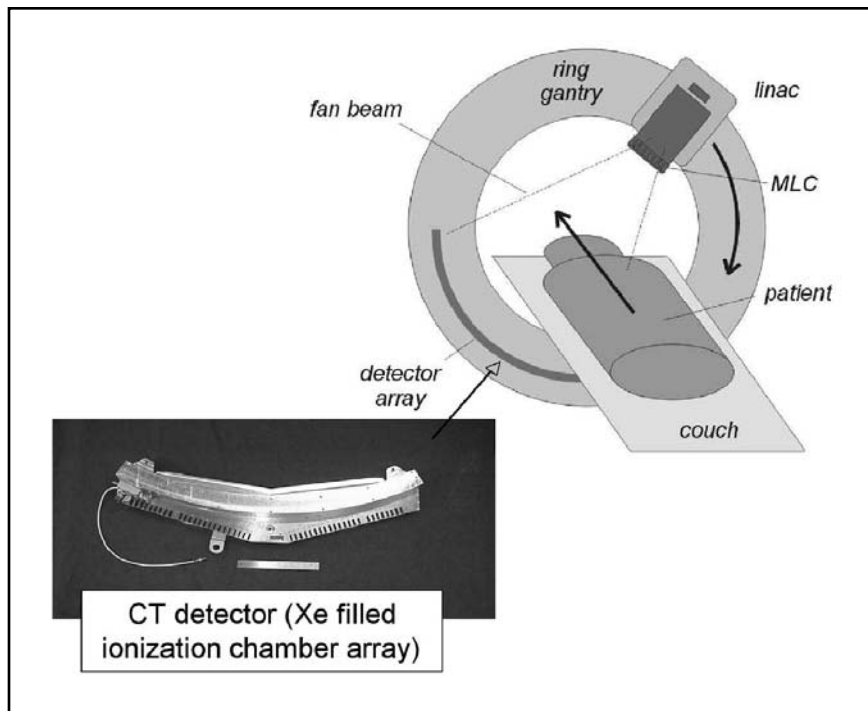


**Figure 12.11:** Illustration of a fan beam CT acquisition principle as used by the TomoTherapy device. The x-ray source and detector array rotate  $360^\circ$  because in a conventional fan beam CT a narrow slit (in the superior-inferior direction) is used; this reduces scatter effects. The MV beam reduces bone contrast. The closed gantry design ensures no restriction on rotation time. SEE COLOR PLATE 54.

- v) *MV cone-beam CT imaging.* Images are acquired using the linac beam and the existing EPID rotated around the patient. Reasonable quality images can be obtained (see Pouliot et al. 2005), though generally with a higher dose than with kilovoltage cone-beam imaging. The vendor that offers this option is Siemens.
- iv) *Fan-beam MV CT.* The TomoTherapy Hi-Art System<sup>®</sup> uses a megavoltage beam and a conventional CT detector to collect CT images before each treatment (see figure 12.11). Unlike the methods described in (iii) and (v) a fan-beam geometry rather than a cone-beam geometry is used for imaging.

Both MV CT devices offer an advantage when scanning patients with hip prostheses or dental fillings because the high Z material does not produce an artifact at megavoltage energies (see figure 12.12).

There are two other modalities that also offer imaging of the internal anatomy with no extra ionizing radiation due to their imaging mode; these are:

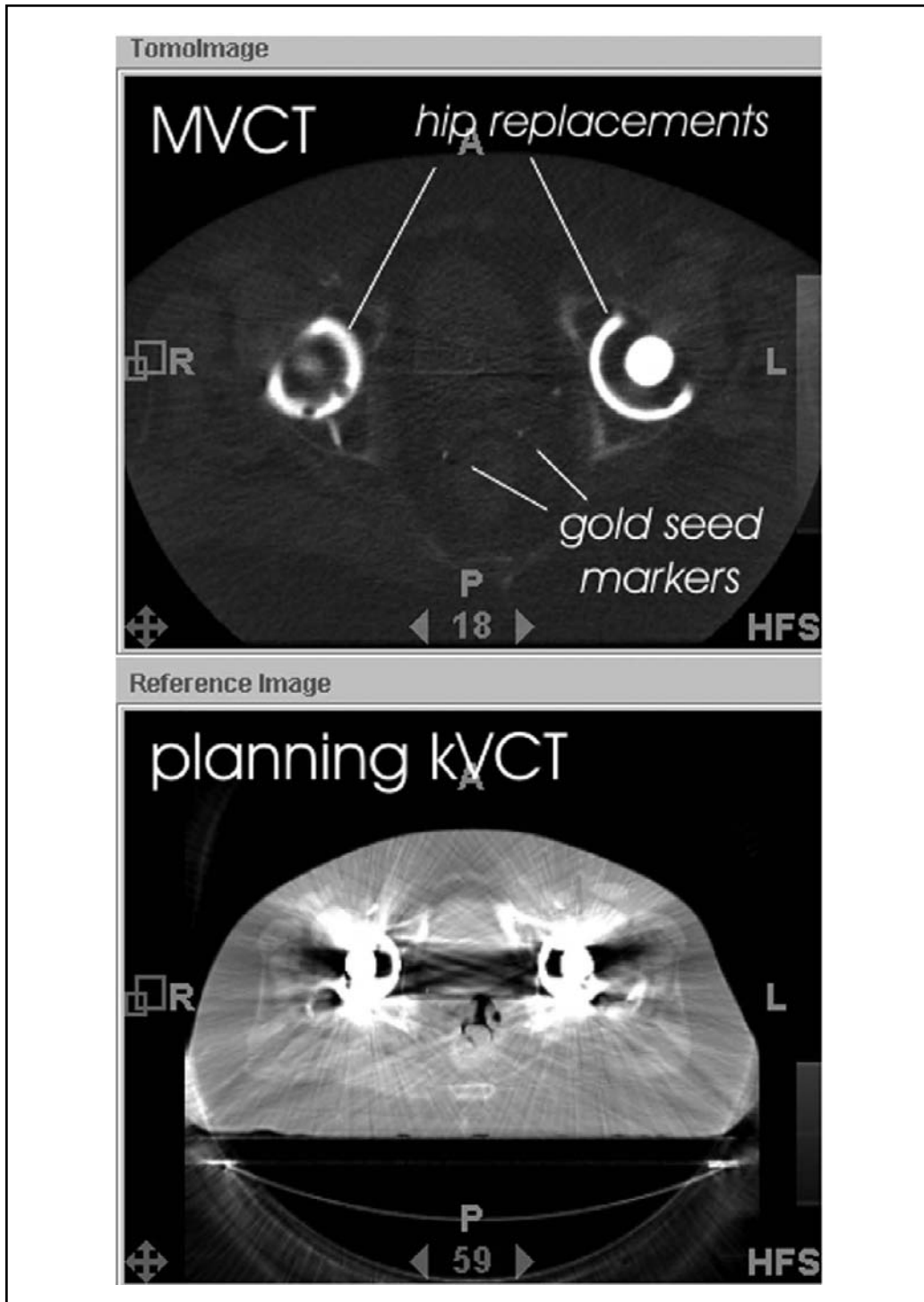


**Figure 12.12:** Comparison of a MV CT image acquired using the TomoTherapy device and a kV CT image collected using a conventional kV CT of a patient with dual hip replacements. The patient had gold fiducial markers implanted in the prostate and seminal vesicles.

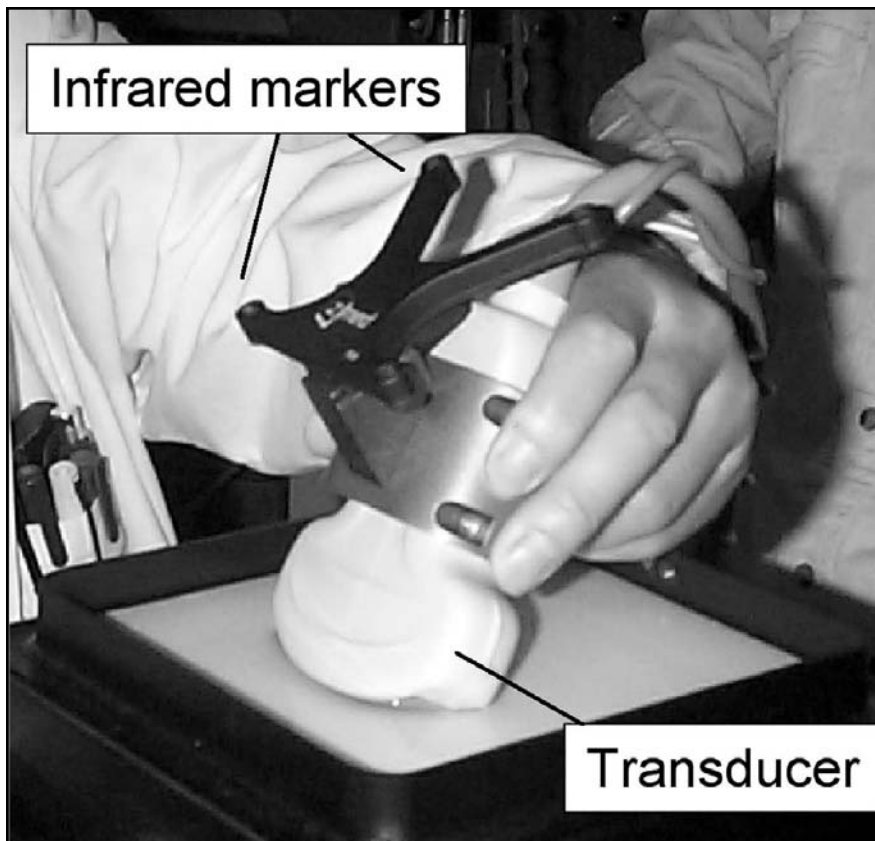


**Figure 12.13:** Ultrasound probe used for positioning of prostate in the treatment room prior to linac treatment delivery. The exact location of this probe is determined using two infrared cameras. The combination of many 2-D ultrasound images also allows reconstruction of 3-D images. (Courtesy of London Regional Cancer Program, Canada.)

- i) *Ultrasound*, which has been used for in-room verification for prostate position for some time (see also chapter six). An example of such a device is shown in figure 12.13. Ultrasound has been shown to be extremely useful in tracking prostate shifts. The types of images which can be collected using ultrasound are shown in figure 12.14.

The position of the prostate, as determined by the transabdominal ultrasound imaging, is compared to the previously CT-defined prostate location relative to isocenter. The position of the ultrasound transducer is referenced to the coordinate system of the linac's isocenter, either through physical connection to the gantry, or alternately via an infrared localizing system (Tomé et al. 2002). Typically it is the interface regions between the bladder and prostate and the rectum and prostate which show on ultrasound that are used as reference landmarks. The locations of these interfaces relative to isocenter are compared to the planned location, and the necessary calculated couch shifts relocate the prostate to the correct position.

There have been several studies into the use of transabdominal imaging for tracking prostate motion (e.g., Jani et al. 2005, Lattanzi et al. 2000). The technique allows for the daily relocation of the prostate in an attempt to better cover the mobile prostate organ, leading to potential reduction in the target margin. At the very least ultrasound has pioneered our knowledge base about prostate movements. Some user training is required to use these devices effectively. These devices produce no hazard from additional dose from ionizing radiation for image collection, which is an advantage. Tomé has also suggested prostate treatment of post-prostatectomy patients can also be better located using one of these devices; they used the visualization of the bladder neck as a localization reference for the prostatic fossa (Chinnaiyan et al. 2003).

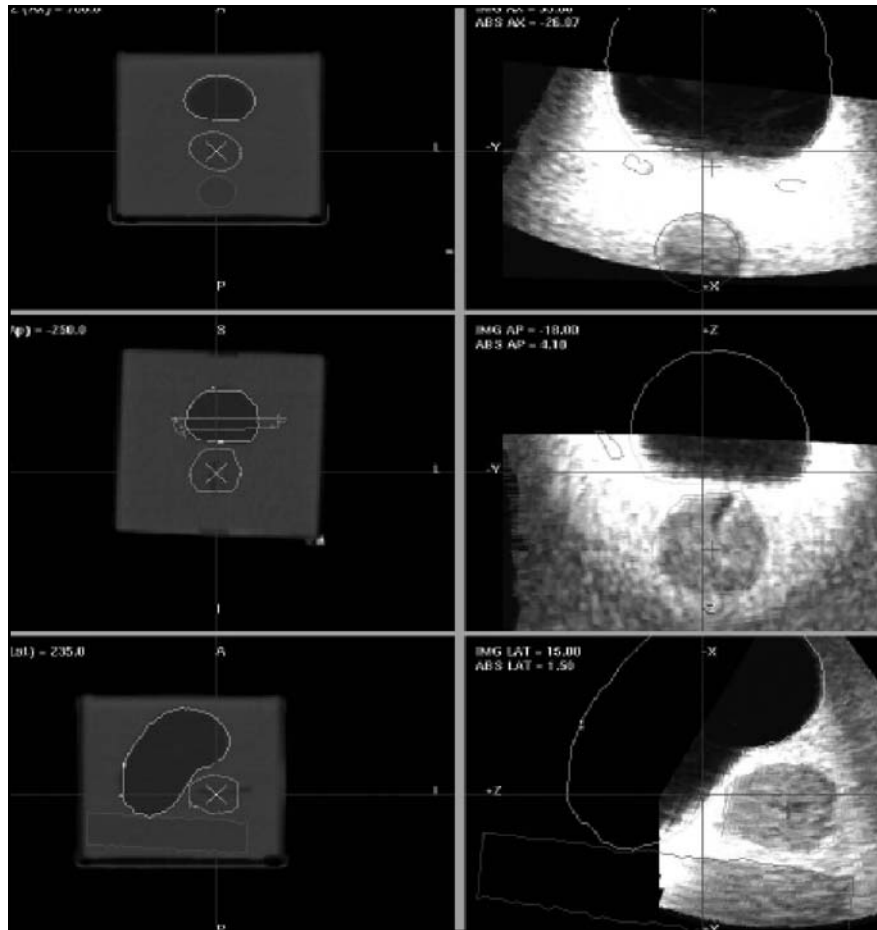


**Figure 12.14:** Three-dimensional reference image (CT, on the left) and ultrasound image of a prostate phantom. (Courtesy of London Regional Cancer Program, Canada.) SEE COLOR PLATE 55.

- ii) *Magnetic resonance imaging (MRI)* is really the most exciting new modality that is being investigated as an in-linac room or MRI LMID option. There are devices that have been suggested such as the one shown in figure 12.15. This design envisages two cobalt-60 sources, each with a binary multileaf collimator (MLC) sandwiched between high magnetic field strength magnets for collection of MRI information during or just after radiotherapy treatment.

A similar machine called the Renaissance™ (ViewRay, Inc.) is being planned by Dempsey and collaborators. This has three cobalt-60 beam sources, each mounted in its own treatment head, with conventional MLC. The multiple source cobalt-60 heads ensure dose rates approaching those currently provided by linacs. It is suggested the simplicity of a cobalt-60 source drive would reduce the impact of the magnetic field from the MRI on the beam steering.

There are also linac-mounted designs using lower strength magnetic fields. Images from these devices have been reported in the literature (Raaymakers et al. 2004). Electrons generated from x-rays are obviously changed in the tracks they follow and this can have large effects on the dose distribution if large magnetic fields are employed (Bielajew 1993). However at these low magnetic field strengths smaller effects on the linac beam dose distributions have been characterized (Raaijmakers et al. 2005).

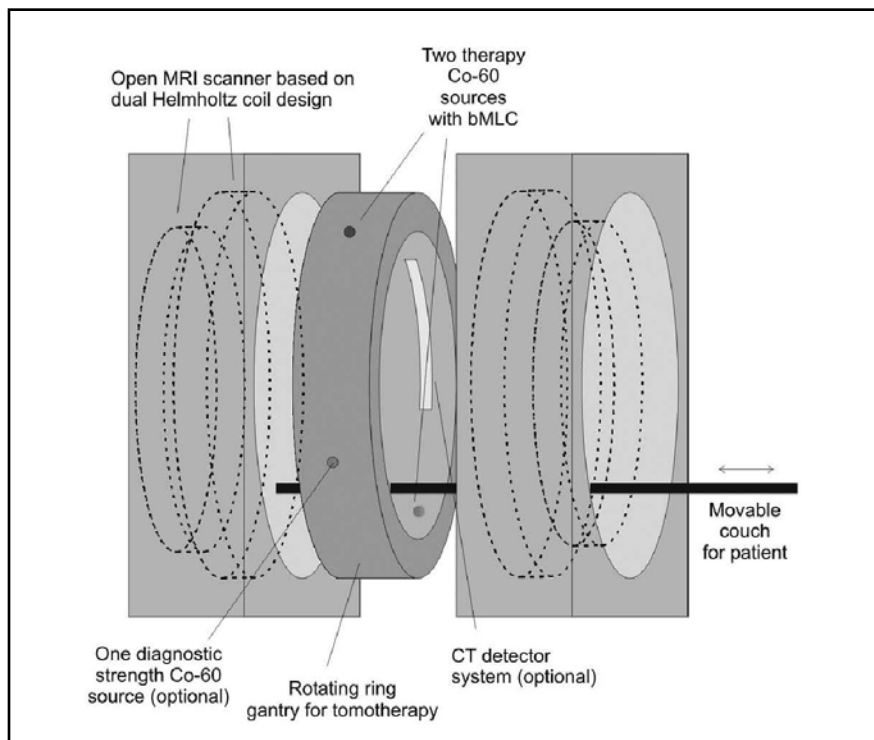


**Figure 12.15:** Schematic illustration of a suggested design for a cobalt-60 unit combined with an MRI scanner (adapted from Kron et al. 2006). This unit design had two cobalt-60 sources, each with a binary MLC sandwiched between MRI scanner magnets.

**Table 12.2:** Comparison of image guidance modalities. Note this is a suggestion for illustration purposes only, as a more tailored evaluation depends on the environment and needs of the user.

	<i>Ultra-sound</i>	<i>EPI</i>	<i>kV Imaging</i>	<i>CT (in room)</i>	<i>CBCT</i>	<i>MVCT</i>	<i>MRI</i>
Imaging dimensions	2 or 3	2	2 plus two orthogonal	3	3	3	3
Image quality	+	+	++	++++	+++	+++	++++
Soft tissue contrast	+++		+	++	++	+	+++
Field verification	no	yes	no	no	no	no	no
Dose reconstruction		+		+	+	+++	
Dose (cGy)	none	3	0.3	2	2	2	none
Time per patient (min.)	5	1	3	5	5	5	not known
Feasibility/ease of use	training required	easy	easy	large bunker	--	--	not tested
Cost	low	low	medium	high	high	medium	very high

Most of these various competing linac-mounted, or in-linac room, imaging modalities are very new to the market; some are still just designs. Early comparisons such as in table 12.2 give estimates only of the relative merits of each device.

## 12.5 Intrafraction Motion Management

Intrafraction variation is due to a change in patient geometry during the dose delivery within a treatment fraction, often caused by involuntary internal organ motion. Skeletal, gastrointestinal, and cardiac systems all contribute to intrafraction motion; however, it is respiratory motion towards which significant research and development have been directed (Keall et al. 2006a,b). This may be attributed to the extent of tumor movement caused by respiratory motion; lung and thoracic tumors moving as much as 5 cm during respiration have been reported (Keall et al. 2006a,b). More typical movements may be in the order of 1 to 2 cm; however the actual extent of motion depends very much on where the tumor is located in the lung—in general, peripheral tumors move less.

Large margins are necessary in the PTV to account for the limits of tumor motion. These increased margins in turn lead to the volume of normal tissue irradiated being larger, and this may be associated with a necessary reduction in prescribed dose. It is also suggested that breathing leads to a spreading out of the dose distribution during radiation delivery, resulting in a deviation between the intended dose and the dose delivered (Li et al. 2006). Methods which specifically account for respiratory motion include:

- i) Motion encompassing volume, this may involve 4DCT of respiratory volume or inhale-exhale breath-hold (see figure 12.16a).
- ii) Respiratory gating (see figure 12.16b).
- iii) Motion adaptive therapy known as tumor tracking (see figure 12.16c).

### 12.5.1 Gating

Respiratory gating during imaging allows selected portions of the breathing waveform to be reconstructed between specified time intervals or specified amplitudes. Gated delivery only treats in a selected portion, or *gate*, thus reducing tumor movement when the beam is on by providing a series of snapshots of tumor treatment tuned to the respiratory cycle.

Optimally, because the gate has finite and necessary time width to achieve a reasonable dose rate, this would be chosen where tumor motion is the least,

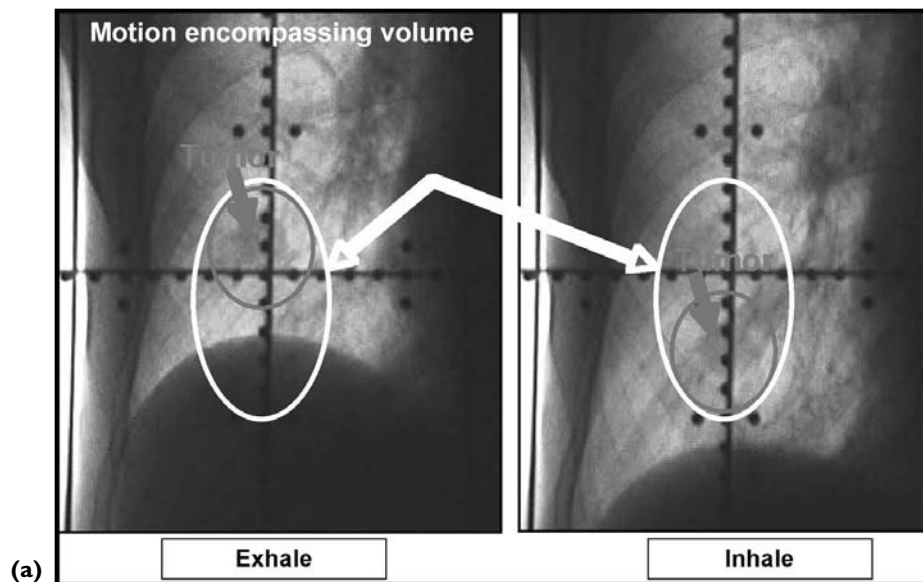


**Figure 12.16:** Strategies for dealing with intrafraction motion: (a) Motion encompassing volume; this may involve 4DCT of respiratory volume or inhale-exhale breath-hold; (b) Respiratory gating involving beam-hold off and beam-on during selected phases of the respiration cycle; (c) Motion adaptive therapy known as tumor tracking, whereby a device such as a DMLC follows (tracks) the tumor target motion during beam-on. (Courtesy of P. Keall, Stanford University.) SEE COLOR PLATE 56.

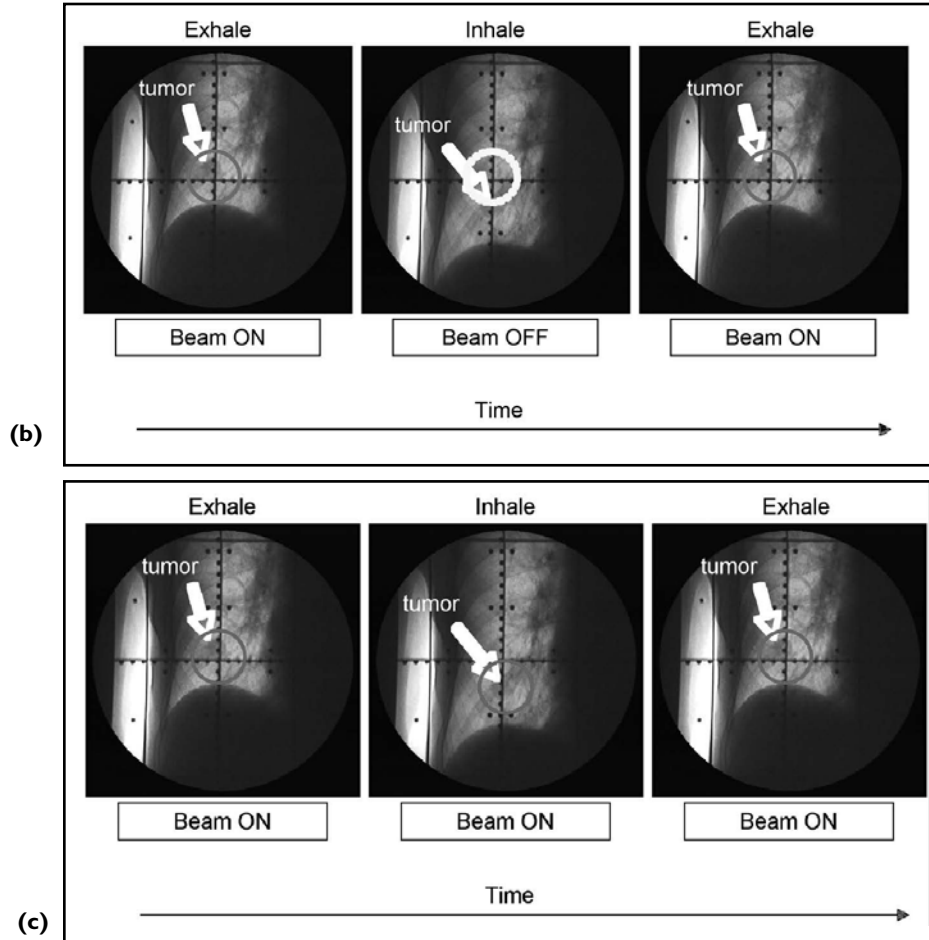
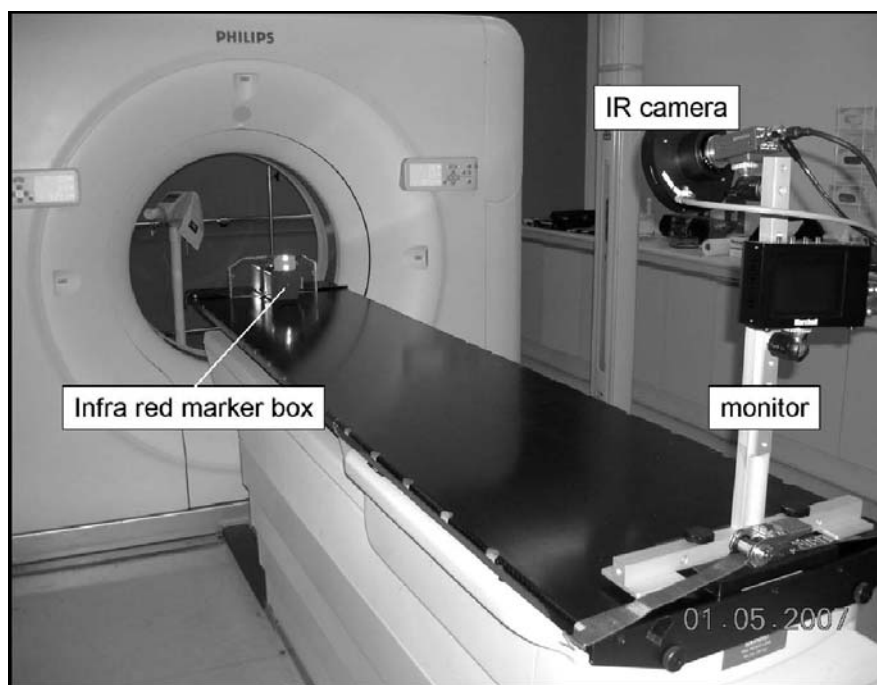


**Figure 1.16:** (Continued.) SEE COLOR PLATE 57.

perhaps end expiration. Another option might be at end inspiration where lung volume is maximal, often separating the tumor from critical structures such as the heart and spinal cord (Keall et al. 2006a,b). The choice of gate width must be a compromise between the time the beam is on as a ratio of the total treatment time, the *duty cycle*, and the amount of tumor motion within the gate, *tumor residual motion*. Treatment delivery time is typically increased up to threefold using respiratory gating due to the average duty cycle for treatment ranging from 30% to 50% (Jiang 2006).

Real-time knowledge of the tumor position is necessary in all methods accounting for intrafraction motion. Respiration monitoring techniques include internal fiducial-based methods, and externally based surrogate methods. Surrogate methods rely on external surrogates such as reflective skin markers or lung air volume measurements corresponding to internal tumor motion. Internal fiducial-based methods rely on on-line fluoroscopic or electronic portal imaging to directly detect the location of the tumor through implanted fiducials.

There are several commercially available respiratory gating systems that utilize external surrogates for tumor motion. One such system is the *real-time position management (RPM)* system. The RPM system (Varian Medical Systems) uses a video camera to detect the motion of external infrared reflecting markers. Figure 12.17a shows the RPM respiratory gating system coupled with a Philips CT. *Four-dimensional CT (4DCT)* is produced by oversampled data acquisition at each slice. Multiple images can then be reconstructed per slice and are evenly distributed over the acquisition time. Each of these images represents a different anatomical state of the breathing cycle. Reconstructed images can then be sorted into spatio-temporally coherent volumes based on respiratory phase as discerned by the external surface marker (Reitzel et al. 2005). Figure 12.17b shows the plastic marker box with two infrared-reflecting markers placed on the patient's chest between the umbilicus and xiphoid. The infrared markers are illuminated by infrared light-emitting diodes, and images of the markers are captured by



(a)

**Figure 12.17:** The real-time position management (RPM) system (vendor, Varian Medical Systems). The RPM system uses a video camera to detect the motion of external infrared reflecting markers: (a) RPM respiratory gating system coupled with a Philips CT. 4DCT images are produced by oversampled data acquisition at each slice; (b) Plastic marker box with infrared markers placed on the abdomen of patient for motion detection by infrared camera; (c) The image in the top left-hand corner displays the real-time video footage of marker motion, while the image in the bottom right-hand corner displays the motion track. The gated portions of the breathing cycle, or beam-on pulses, can be seen below the respiratory waveform. During treatment on the linac, a signal to the gun allows treatment only when motion is within the gate.

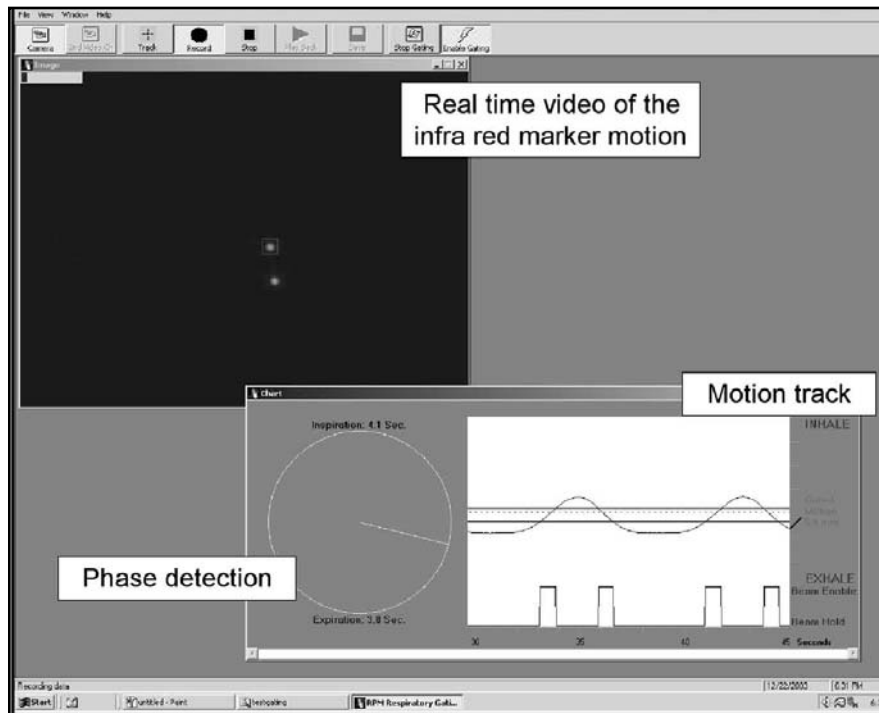
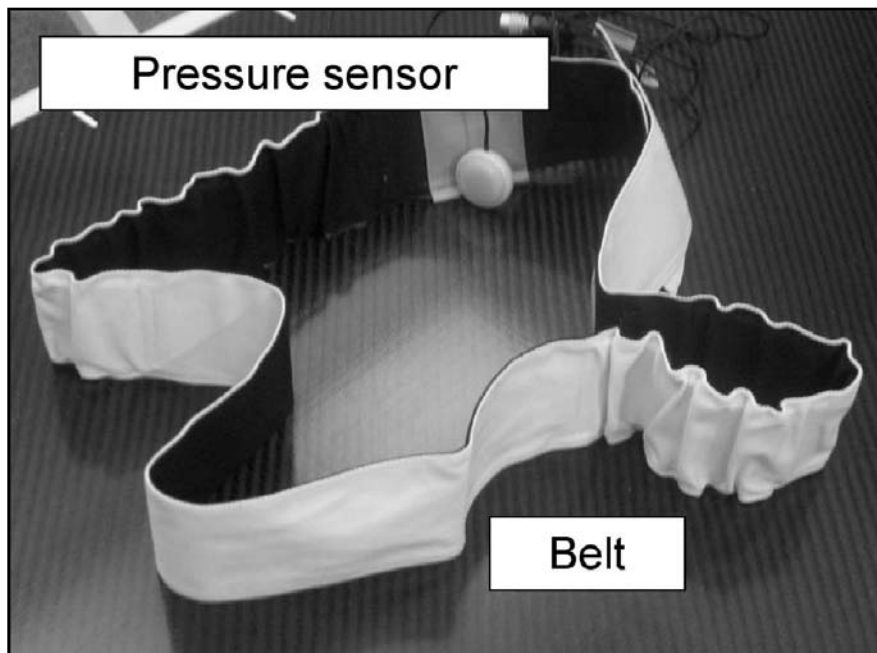


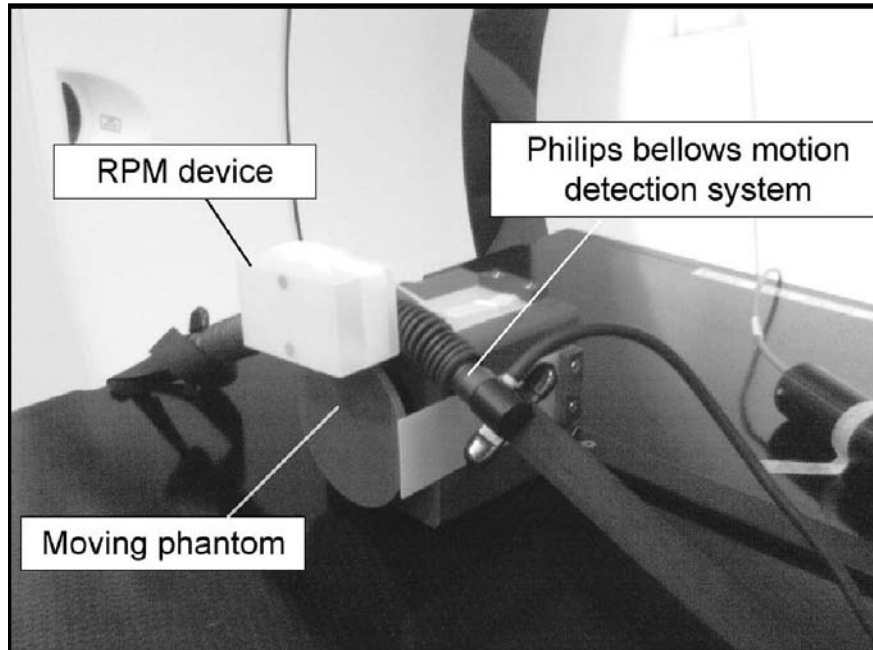
Figure 12.17: (Continued.)

the camera at 30 frames per second. The camera output is directed to a PC running the RPM software; a tracking algorithm establishes the amplitude and period of the motion. The software designates end-inhale and end-exhale positions and assigns phases by linear interpolation (Rietzel et al. 2005). The user interface can be seen in figure 12.17c. The image in the top left-hand corner displays the real-time video footage of marker motion, while the image in the bottom right-hand corner displays the motion track. The gated portions of the breathing cycle, or beam-on pulses, can be seen below the respiratory waveform. During treatment on the linac, a signal from the PC to the grid gun allows treatment only when motion is within the gate (Yorke et al. 2005). Patient internal anatomy positioning during treatment should be verified using in-room imaging before treatment, and marker block position and patient breathing waveform should be as close as possible to that obtained in planning.

Another commercial gating system is based on a pressure belt feedback mechanism; the Anzai belt (AZ-733V by Anzai Medical) is used by Siemens 4DCTs and linacs. This is depicted in figure 12.18a and consists of an elastic belt containing a load cell which detects external respiratory motion in real-time through changes in abdominal motion. The signal from the load cell is amplified and fed into the scanner. As the patient breathes in, the belt tight-



**Figure 12.18:** Two other commercial system approaches to monitoring the breathing cycle: (a) The Anzai belt (model AZ-733V, vendor Anzai Medical), used by Siemens 4DCT and linac devices. This consists of an elastic belt containing a load cell which detects external respiratory motion in real-time through changes in abdominal motion. As the patient breathes in, the belt tightens and pressure is exerted on the load cell; thus a higher amplitude signal is produced. A decreasing in amplitude of the signal corresponds to the exhalation respiratory phase.



(b)

**Figure 12.18:** (Continued.) Two other commercial system approaches to monitoring the breathing cycle: (b) A bellows system (Philips) shown with the RPM system (Varian) on a phantom; it is important to correlate two different systems if one is to be used for 4DCT acquisition and the other for treatment delivery gating.

ens and pressure is exerted on the load cell; thus a higher amplitude signal is produced. A decreasing in amplitude of the signal corresponds to the exhalation respiratory phase.

The belt is connected to the sensor port, which is in turn connected to the wave deck. The system is run by a PC which offers a graphical user interface for monitoring and recording the signal. During spiral CT mode respiratory data are acquired during a whole helical CT scan and stored. Projections are integrated over a 250 ms window, starting from a given phase. The Anzai belt recognizes the lowest amplitude phase point (0% inhalation) and the highest amplitude phase point (100% inhalation). In-between phases for inhalation are calculated by linear scaling. Similarly, the peak of the curve (maximum amplitude) is recognized as 0% exhalation and the trough, 100% exhalation with in-between phases calculated by linear scaling. Yet another system using a bellows approach is implemented by Philips (see figure 12.18b).

Another issue is that although motion artifacts are reduced in 4DCT, they still exist. Each phase of retrospective re-binning is a snapshot of regular respiration and is subject to artifacts due to incorrect phase determination or an irregular breathing pattern. Motion intraphase will also produce artifacts due to the partial projection effect and this must be taken into account in planning (Rietzel et al. 2005).

Gated linac treatment using the Anzai belt follows the same principle as the RPM respiratory gating system, where the beam is only triggered at pre-determined portions of the respiratory cycle. If at any stage, breathing becomes erratic, such as the patient coughing, the system is designed to automatically switch off. Design of phantoms which test the effectiveness of these devices during the treatment cycle are really in their infancy; usually an existing phantom is modified to move in 1-D or 2-D (as an example see figure 12.19).

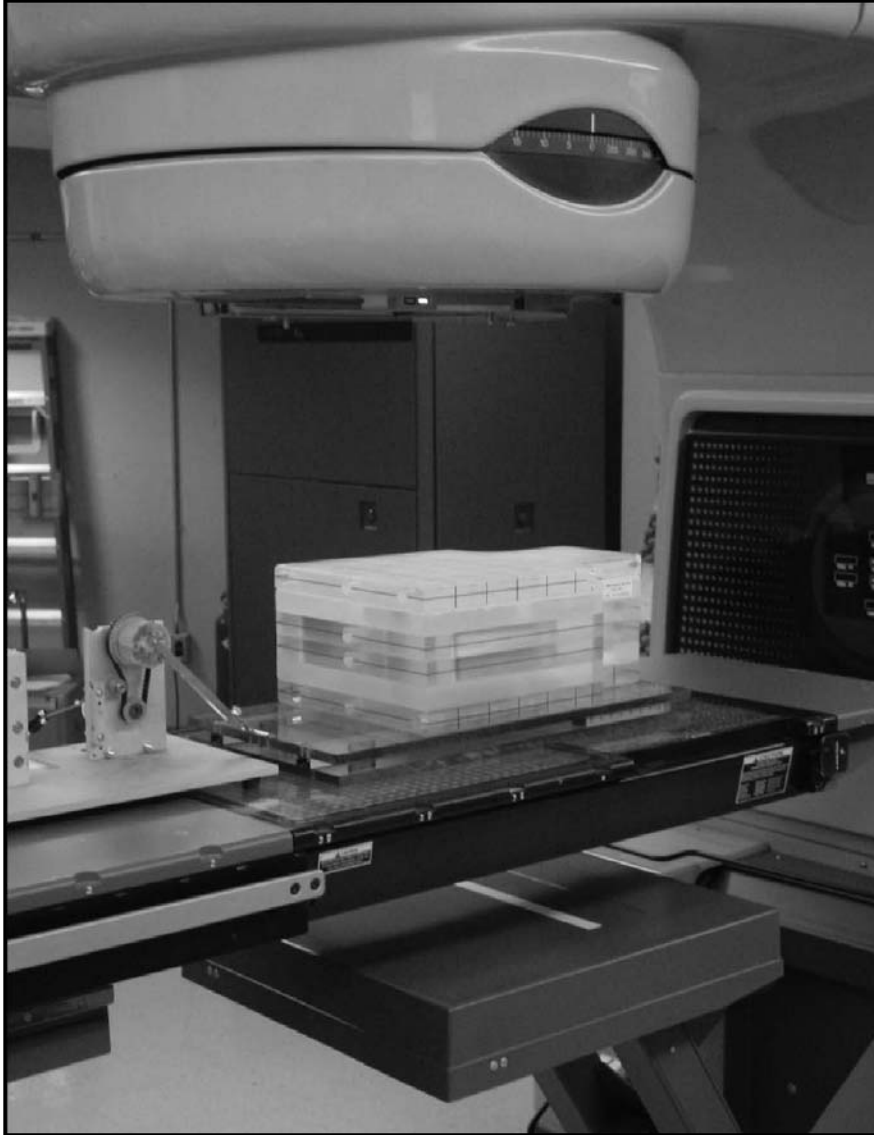


**Figure 12.19:** Commercial dosimetry phantom (Standard Imaging Ltd.) moving on rails driven by a rotating arrangement. (Courtesy of P. Keall, Stanford University.)

Respiratory gating using external surrogates is noninvasive, and allows the patient to breathe freely during both planning and treatment. Patients chosen should have fairly stable breathing, and reasonably large intrafraction tumor motion, so as to benefit from treatment because a reduced target volume can be specified. Studies have shown that respiratory training and visual and audio feedback can improve respiratory reproducibility for gating purposes (e.g., Jiang 2006). External surrogates rely heavily on internal tumor motion correlating with the motion of the external marker, which may not always be the case.

Internal-based fiducial gating utilizes fiducial markers detected by radiographic means to gate radiation delivery (Keall et al. 2006a,b). The technique was jointly developed by Hokkaido University and Mitsubishi (Seppenwoolde et al. 2002). Gold seeds are implanted close to the target location, and the fiducial position is tracked in 3-D using a pair of stereotactic kilovoltage x-ray imaging systems with automatic detection software (Keall et al. 2006a,b).

During treatment, the linac is activated when the desired position of the fiducial is obtained for both stereotactic x-ray cameras. Internal-based fiducial methods have the advantage of directly measuring the tumor position by fluoroscopic imaging. However, placement of fiducials for internal-based gating of lung tumors is associated with a high risk of pneumothorax (Jiang 2006).

Patients must also be able to tolerate the implant procedure and remain motionless on the couch for up to 45 minutes (Keall et al. 2006a,b). Fiducial markers can also be loaded by bronchoscope; however fixation and migration of markers in the bronchial tree also pose problems due to the relationship of the markers and the tumor shifting over time (Imura et al. 2005).

## 12.5.2 Breath-hold

*Breath-hold* methods involve the patient holding his or her breath at certain phases of the breathing cycle to reduce tumor movement. Breath-hold methods consist of deep inspiration, active breathing control, or self-held breath-hold.

*Deep inspiration* breath-hold involves coaching the patient to a reproducible maximum inhalation breath-hold during simulation and treatment (Keall et al. 2006a,b). The aim is to immobilize the tumor and to expand healthy lung tissue out of the high-dose region. Control devices used include spirometry and external markers; however they are not used to trigger the linac. The therapist or physicist will observe and record the patient breathing waveforms during simulation and assess multiple breath-holds to establish the reproducibility of the *deep inspiration breath-hold (DIBH)*. CT scans are obtained during free breathing, DIBH, end-inspiration and end-expiration. The free-breathing scan is used for reference, and serves as an alternate treatment plan if DIBH is not feasible for the duration of treatment. End-inspiration and expiration scans give an estimate of tumor motion during normal tidal breathing and can be used for QA purposes. During treatment, the therapist will turn the beam on only when the target breath-hold has been attained and turn the beam off if the breath-hold level falls outside a preset tolerance (Keall et al. 2006a,b).

*Active breathing control (ABC)* is a method used to assist reproducible breath-hold. The ABC spirometry system (Elekta Oncology Systems) enforces patient breath-holds at preselected volumes of respiration during which dose delivery occurs (Wong et al. 1999). The volume of air entering and leaving the lungs is monitored by a spirometer. The changing air volume corresponds to the patient's respiratory signal. The patient breathes normally through the apparatus. The ABC system acquires and controls the desired respiration flow-volume. The operator can activate the software to force a breath-hold for a predetermined period of time by closing the valve of the breathing tube and restricting air flow to and from the patient. The breath-hold is then maintained for 15 to 30 s during treatment, depending on the patient's tolerance (Keall et al. 2006a,b).

There is a *self-held breath-hold* where the patient voluntarily holds his/her breath at some point in the breathing cycle while the prescribed dose is administered. This can occur with or without respiratory monitoring.

Without respiratory monitoring this technique relies on the patient determining when an adequate breath-hold is in place and clearing the interlock by pressing a hand-held switch. This allows the therapist to activate the beam. Releasing the switch asserts the interlock, disabling the beam. Both the therapist and the patient have the power to turn the beam off. The drawback of this method is that it is reliant on a patient's ability to maintain a breath-hold in which internal anatomy is stable for an adequate period of time (>10 s) while controlling the switch. The AAPM report on the management of respiratory motion in radiation oncology (Keall et al. 2006a,b) advises that PTV margins must take into account breath-hold reproducibility, patient setup reproducibility, and internal motion. Due to lack of significant statistical data, margins for internal motion should be tailored to the individual patient by measuring the reproducibility at the simulator session.

*Respiratory monitored self-breath-hold* utilizes an external surrogate such as the RPM system to monitor the breathing waveform and to control dose delivery, while the patient is required to perform a voluntary breath-hold. Similar to the method discussed previously, it is required that the patient can perform a reproducible breath-hold for an adequate period of time and respond to verbal instructions from the therapist. Portal imaging is performed prior to treatment to verify patient positioning. Respiratory monitored self-breath-hold has the safeguard that the waveform is monitored; thus if the breath-hold at any time deviates from predetermined breath-hold margins, the beam will automatically turn off.

Berson et al. (2004) found that breath-hold techniques were beneficial in eliminating possible time lag between tumor and external surrogates, improved diaphragm positional reproducibility and that there was an efficiency gain in CT simulation and treatment (longer duty cycle). Breath-hold methods cannot be used on every patient and are reliant on patient compliance or involuntary restriction of airflow. Treatment is prolonged using breath-holds to account for intrafraction motion as additional time has to be added to enable to patient to recover from each breath-hold.

### 12.5.3 Motion Adaptive Therapy

Motion adaptive therapy consists of respiration-synchronized techniques that shift dose in space to track a tumor's changing position. A dynamic couch, or for small targets, a robotic arm (CyberKnife®, Accuray Inc.) can be used to target a moving tumor's position (Tewatia et al. 2006). 4-D radiotherapy by target tracking has also been proposed (Keall et al. 2004) whereby *dynamic multileaf collimators (DMLCs)* are adjusted to *track* tumor motion.

*CyberKnife®* is an image-guided radiosurgery system in which the linac beam is moved by a robotic arm that is coupled through a real-time loop to an imaging system that monitors tumor location. The robotic arm can move with six degrees of freedom and track the target through a combination of infrared tracking and synchronized x-ray imaging (Schweikard et al. 2003).

Prior to treatment, gold fiducial markers are placed in the vicinity of the target organ. Stereo x-ray imaging is used during treatment to determine the precise spatial location of these markers. The position of internal fiducials is computed repeatedly during treatment through x-ray image processing. In addition to this, infrared emitters are attached to the chest and the abdominal surface of the patient and the infrared tracking system records the motion of these emitters. The software updates and correlates external body surface movement with the movement of internal tumor fiducials. From this correlation model the placement of the internal target can be devised during time intervals where no x-ray images are taken. The beam can be constantly repositioned to account for tumor motion, and dosimetry adapted to allow for changing lung volume.

*DMLC-based motion tracking* is achieved as follows:

- i) 4DCT is used to create separate CT images at discrete phases of the respiratory cycle, which allows temporal anatomic changes over time to be observed.
- ii) Select respiratory phases are reconstructed, and deformable image registration is then performed to map each CT image data set. This allows a representative tumor trajectory to be obtained.
- iii) IMRT treatment planning is simultaneously performed on each CT set reconstructed, and a leaf sequence based on optimized fluence maps is generated.
- iv) The radiation beam defined by the DMLC then tracks the respiration-induced target motion. This is based on a feedback loop including the breathing signal to a real-time MLC controller (Keall et al. 2004). A bench top version of this DMLC device is shown in figure 12.20.

Tewatia et al. (2006) have also researched *breathing synchronized delivery (BSD)* for DMLC-based motion tracking in which the patient is guided to breathe in accordance with target motion obtained from 4DCT data sets. In the case of IMRT, a breathing guide is developed for each patient from his or her normal breathing patterns (obtained from spirometry). The

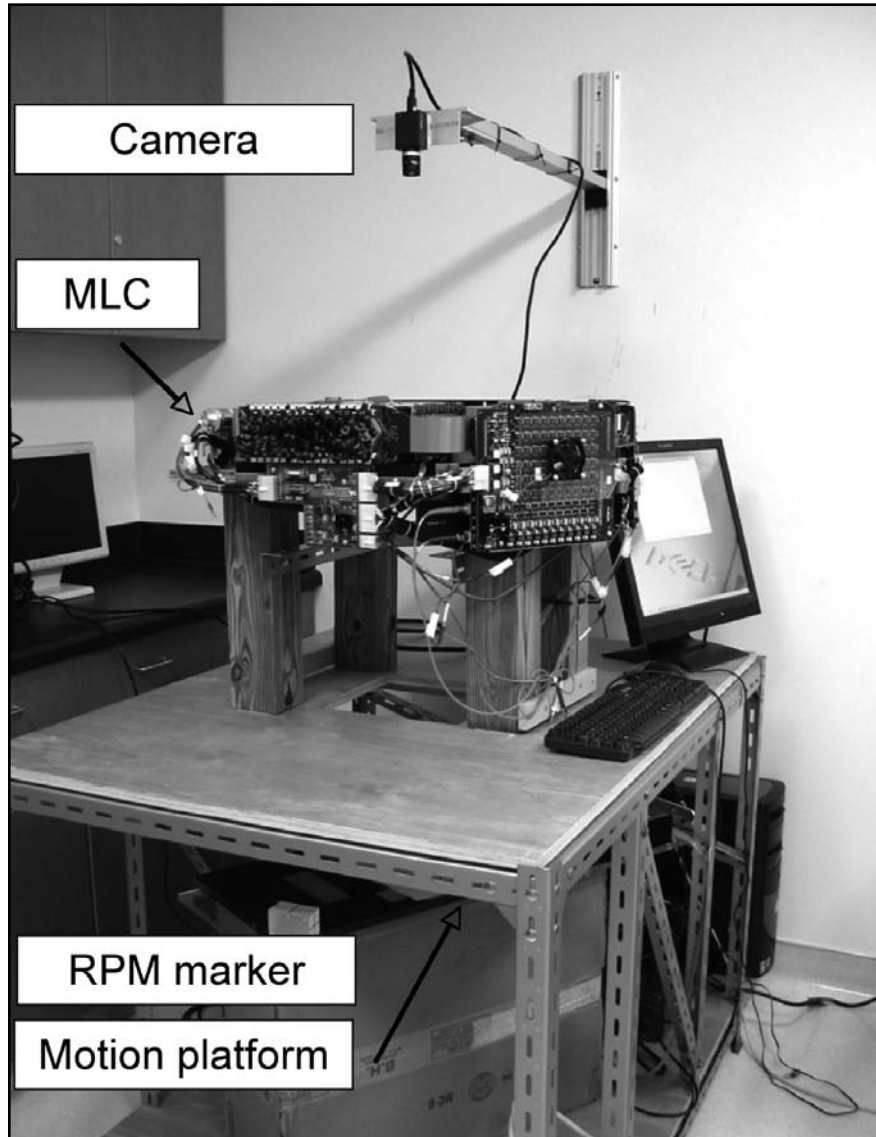


**Figure 12.20:** A bench top version of a DMLC tracking device. The MLC leaves move during beam-on to encompass the target volume which is changing. DMLC tracking is achieved by feedback from the infrared marker. (Courtesy of P. Keall, Stanford University.)

patient is then required to reproduce this breathing cycle by following a visual prompt. 4DCT data sets are then obtained and DMLC planning performed as described previously. It is assumed that the patient maintains a constant breathing cycle and the dose rate from the treatment machine is constant so that the treatment process correlates with the breathing phase. The instantaneous average tumor displacement is overlaid on the DMLC position at corresponding phases and the leaf speed is evaluated to ensure accurate treatment delivery.

The advantages of motion adaptive therapy include:

- i) Accounts for 3-D motion of the tumor.
- ii) The duty cycle for treatment is 100%.

Time delay compensation is necessary for both the CyberKnife and conventional DMLC; a 200 ms delay between acquisition of tumor coordinates and repositioning of the linac is present, in addition to image acquisition, read-out, and processing times (Tewatia et al. 2006). This necessitates prediction algorithms such that the beam can be synchronized at the position of the tumor, which may be difficult if the patient breathes irregularly. Murphey et al. (2002) have found that by using breathing predictions with a variety of adaptive filters, tumor position can be predicted with up to 80% accuracy in the presence of a 200 ms system time delay, but that accuracy degrades rapidly at longer delay intervals. The report also highlights that dosimetric considerations should be taken into account in treating a changing volume. The anatomy and air volume of the lung are continually changing during breathing, which perturbs the attenuation of the treatment beam and alters the position of the tumor with respect to normal tissue and critical structures.

## References

- Berson A., Emery R., Rodriguez L., Richards G.M., Nq T., Sanghavi S., Barsa J. (2004) Clinical experience using respiratory gated radiation therapy: Comparison of free breathing and breath-hold techniques. *Int. J. Radiat. Oncol. Biol. Phys.* 60: 419–426.
- Bielajew A.F. (1993) The effect of strong longitudinal magnetic fields on dose deposition from electron and photon beams. *Med. Phys.* 20: 1171–1179.
- Breen S.L., Craig T., Bayley A., O'Sullivan B., Kim J., Jaffray D. (2006) Spinal cord planning risk volumes for intensity-modulated radiation therapy of head-and-neck cancer. *Int. J. Radiat. Oncol. Biol. Phys.* 64: 321–325.
- Chinnaiyan P., Tomé W., Patel R., Chappell R., Ritter M. (2003) 3D-ultrasound guided radiation therapy in the post-prostatectomy setting. *Technol. Cancer Res. Treat.* 2: 455–462.
- Crook J.M., Raymond Y., Salhani D., Yang H., Esche B. (1995) Prostate motion during standard radiotherapy as assessed by fiducial markers. *Radiother. Oncol.* 37: 35–42.
- Holland R., Veling S.H., Mravunac M., Hendriks J.H. (1985) Histologic multifocality of Tis, T1-2 breast carcinomas. Implications for clinical trials of breast conserving surgery. *Cancer* 56: 979–990.
- Hugo G.D., Yan D., Liang, J. (2007) Population and patient-specific target margins for 4D adaptive radiotherapy to account for intra- and inter-fraction variation in lung tumour position. *Phys. Med. Biol.* 52: 257–274.
- Hysing L.B., Kvinnsland Y., Lord H., Muren L.P. (2006) Planning organ at risk volume margins for organ motion of the intestine. *Radiother. Oncol.* 80: 349–354.
- ICRU (International Commission on Radiation Units and Measurements) (2004) Report 71, Prescribing, recording, and reporting electron beam therapy. ICRU, Bethesda, Maryland.
- ICRU (International Commission on Radiation Units and Measurements) (2001) Report 64, Dosimetry of high-energy photon beams based on standards of absorbed dose to water. ICRU Bethesda, Maryland.

- ICRU (International Commission on Radiation Units and Measurements) (1999) Report 62: Prescribing, recording, and reporting photon beam therapy (Supplement to ICRU Report 50). ICRU, Bethesda, Maryland.
- ICRU (International Commission on Radiation Units and Measurements) (1998) Report 58: Dose and volume specification for reporting interstitial brachytherapy. ICRU, Bethesda, Maryland.
- ICRU (International Commission on Radiation Units and Measurements) (1993) Report 50: Prescribing, recording, and reporting photon beam therapy. ICRU, Bethesda, Maryland.
- ICRU (International Commission on Radiation Units and Measurements) (1985) Report 38: Gynaecological brachytherapy. ICRU, Bethesda, Maryland.
- Imura M., Yamazaki K., Shirato H., Onimaru R., Fujino M., Shimizu S., Harada T. et al. (2005) Insertion and fixation of fiducial markers for setup and tracking of lung tumors in radiotherapy. *Int. J. Radiat. Oncol. Biol. Phys.* 63: 1442–1447.
- Jani A., Gratzle J., Muresan E., Martel M. (2005) Impact on late toxicity of using transabdominal ultrasound for prostate cancer patients treated with intensity modulated radiotherapy. *Technol. Cancer Res. Treat.* 4: 115–120.
- Jiang S.B. (2006) Technical aspects of image-guided respiration-gated radiation therapy. *Med. Dosim.* 31: 141–151.
- Jin J.Y., Ajlouni M., Chen Q., Yin F.F., Movsas B. (2006) A technique of using gated-CT images to determine internal target volume (ITV) for fractionated stereotactic lung radiotherapy. *Radiother. Oncol.* 78: 177–184.
- Keall P.J., Mageras G.S., Balter J.M., Emery R., Forster K.M., Jiang S.B., et al. (2006a) The management of respiratory motion in radiation oncology report of AAPM Task Group 76. *Med. Phys.* 33: 3874–3900.
- Keall P.J., Vedam S., George R., Bartee C., Siebers J., Lerma F., Weiss E., Chung T. (2006b) The clinical implementation of respiratory gated intensity-modulated radiotherapy. *Med. Dosim.* 31: 153–162.
- Keall P.J., Joshi S., Vedam S.S., Siebers J.V., Kini V.R., Mohan R. (2004) Four-dimensional radiotherapy planning for DMLC-based respiratory motion tracking. *Med. Phys.* 32: 942–951.
- Knoos T., Kristensen I., Nilsson P. (1998) Volumetric and dosimetric evaluation of radiation treatment plans: radiation conformity index. *Int. J. Radiat. Oncol. Biol. Phys.* 42: 1169–1176.
- Kron T., Eyles D., Schreiner J., Battista J. (2006) Magnetic resonance imaging for adaptive cobalt tomotherapy: A proposal. *J. Med. Phys. (India)* 31: 238–250.
- Lattanzi J., McNeely S., Donnelly S., Palacio E., Hanlon A., Schultheiss T.E., Hanks G.E. (2000) Ultrasound-based stereotactic guidance in prostate cancer-quantification of organ motion and set-up errors in external beam radiation therapy. *Comput. Aided Surg.* 5: 289–295.
- Li X.A., Stepaniak C., Gore E. (2006) Technical and dosimetric aspects of respiratory gating using a pressure-sensor motion monitoring system. *Med. Phys.* 33: 145–153.
- Little D.J., Dong L., Levy L.B., Chandra A., Kuban D.A. (2003) Use of portal images and BAT ultrasonography to measure setup error and organ motion for prostate IMRT: Implications for the treatment margins. *Int. J. Radiat. Oncol. Biol. Phys.* 56: 1218–1224.
- Lorchel F., Dumas J.L., Noel A., Wolf D., Bosset J.F., Aletti P. (2006) Esophageal cancer: determination of internal target volume for conformal radiotherapy. *Radiother. Oncol.* 80: 327–332.
- Muren L.P., Karlsdottir A., Kvinnsland Y., Wentzel-Larsen T., Dahl O. (2005) Testing the new ICRU 62 ‘Planning Organ at Risk Volume’ concept for the rectum. *Radiother. Oncol.* 75: 293–302.
- Murphey M., Jalden J., Isaksson M. (2002) Adaptive filtering to predict lung tumor breathing motion during image-guided radiation therapy. *Proceedings of the 16th International Congress on Computer-assisted Radiology and Surgery (CARS)*. pp 539–544.

- Nederveen A.J., Dehnad H., van der Heide U.A., van Moorselaar R.J., Hofman P., Lagendijk J.J. (2003) Comparison of megavoltage position verification for prostate irradiation based on bony anatomy and implanted fiducials. *Radiother. Oncol.* 68: 81–88.
- Pouliot J., Bani-Hashemi A., Chen J., Svatos M., Ghelmansarai F., Mitschke M., Aubin M., Xia P., et al. (2005) Low-dose megavoltage cone-beam CT for radiation therapy. *Int. J. Radiat. Oncol. Biol. Phys.* 61:1 552–560.
- Raaijmakers A.J., Raaymakers B.W., Lagendijk J.J. (2005) Integrating a MRI scanner with a 6 MV radiotherapy accelerator: Dose increase at tissue-air interfaces in a lateral magnetic field due to returning electrons. *Phys. Med. Biol.* 50: 1363–1376.
- Raaymakers B.W., Raaijmakers A.J., Kotte A.N., Jette D., Lagendijk J.J. (2004) Integrating a MRI scanner with a 6 MV radiotherapy accelerator: dose deposition in a transverse magnetic field. *Phys. Med. Biol.* 49: 4109–4118.
- Rietzel E., Liu A.K., Doppke K.P., Wolfgang J.A., Chen A.B., Chen G.T., Choi N.C. (2006) Design of 4D treatment planning target volumes. *Int. J. Radiat. Oncol. Biol. Phys.* 66: 287–295.
- Rietzel E., Pan T., Chen G.T. (2005) Four-dimensional computed tomography: image formation and clinical protocol. *Med. Phys.* 32: 874–889.
- Schweikard A., Shiomi H., Adler J. (2004) Respiration tracking in radiosurgery. *Med. Phys.* 31: 2738–2741.
- See A., Kron T., Johansen J., Hamilton C., Bydder S.A., Hawkins J., Roff M., Denham J.W. (2000) Decision-making models in the analysis of portal films: a clinical pilot study. *Australas. Radiol.* 44: 72–83.
- Seppenwoolde Y., Shirato H., Kitamura K., Shimizu S., van Herk M., Lebesque J.V., Miyasaka K. (2002) Precise and real-time measurement of 3-D tumor motion in lung due to breathing and heartbeat, measured during radiotherapy. *Int. J. Radiat. Oncol. Biol. Phys.* 53: 822–834.
- Stroom J., Heijmen B.J. (2006) Limitations of the planning organ at risk volume (PRV) concept. *Int. J. Radiat. Oncol. Biol. Phys.* 66: 279–286.
- Tewatia D., Zhang T., Tomé W., Paliwal B., Metha M. (2006) Clinical implementation of target tracking by breathing synchronized delivery. *Med. Phys.* 33: 4330–4336.
- Tomé W.A., Meeks S.L., Orton N.P., Bouchet L.G., Bova F.J. (2002) Commissioning and quality assurance of an optically guided three dimensional ultrasound target localization system for radiotherapy. *Med. Phys.* 29:1781–1789.
- van Herk M., Remeijer P., Rasch C., Lebesque J.V. (2000) The probability of correct target dosage: dose-population histograms for deriving treatment margins in radiotherapy. *Int. J. Radiat. Oncol. Biol. Phys.* 47:1121–1135.
- Wong J.W., Sharpe M.B., Jaffray D.A., Kini V.R., Robertson J.M., Stromberg J.S., Martinez A.A. (1999) The use of active breathing control (ABC) to reduce margin for breathing motion. *Int. J. Radiat. Oncol. Biol. Phys.* 44: 911–919.
- Wu J., Haycocks T., Alasti H., Ottewell G., Middlemiss N., Abdoell M., Warde P., Toi A., Catton C. (2001) Positioning errors and prostate motion during conformal prostate radiotherapy using on-line isocentre set-up verification and implanted prostate markers. *Radiother. Oncol.* 61:127–133.
- Yorke E., Rozenweig K.E., Wagman R., Mageras G.S. (2005) Interfractional anatomic variation in patients treated with respiration-gated radiotherapy. *J. Appl. Clin. Med. Phys.* 6: 19–32.
- Zelefsky M.J., Crean D., Mageras G.S., Lyass O., Happersett L., Ling C.C., Leibel S.A., Fuks Z., Bull S., Kooy M., van Herk M., Kutcher G.J. (1999) Quantification and predictors of prostate position variability in 50 patients evaluated with multiple CT scans during conformal radiotherapy. *Radiother. Oncol.* 50: 225–234.

## Questions

- 12.1** If the internal margin is 3 mm and the set-up margin is 4 mm, calculate the margin between CTV and PTV.  
(section 12.2)
- 12.2** Using the van Herk recipe (equation 12.3) calculate the margin if the systematic movement error is assessed as 2 mm and the random movement error as 3 mm.  
(section 12.2)
- 12.3** Name two considerations when considering implementing a patient immobilization device.  
(section 12.3)
- 12.4** Name three treatment strategy options now that 4DCT images showing surrogate tumor movement during the respirator cycle are available.  
(section 12.5)
- 12.5** Describe some of the technical challenges facing the implementation of tumor tracking of lung tumors.  
(section 12.5)